SUPPORTING INFORMATION

Selective degradation of MLK3 by novel CEP1347-VHL-02 PROTAC compound limits the oncogenic potential of TNBC

Kamila Karpińska,[1, 6] Dawid Mehlich,[1, 2, 6] Venkata R. Sabbasani,[3] Michał Łomiak,[1] Pedro Torres-Ayuso,[4] Katarzyna Wróbel,[1] Vi Nguyen-Phuong Truong[1], Remigiusz Serwa,[5] Rolf E. Swenson,[3] John Brognard,[2,*] and Anna A. Marusiak[1, *]

[1]Laboratory of Molecular OncoSignalling, IMol Polish Academy of Sciences, 02-247, Warsaw, Poland

[2]Laboratory of Cell and Developmental Signaling, National Cancer Institute, National Institutes of Health, Frederick, MD 21702, USA

[3]Chemistry and Synthesis Center, National Heart Lung and Blood Institute, National Institutes of Health, Bethesda, MD 20892, USA

[4]Department of Cancer and Cellular Biology, Lewis Katz School of Medicine, Temple University, Philadelphia, PA 19140, USA

[5]Proteomic Core Facility, IMol Polish Academy of Sciences, 02-247, Warsaw, Poland

[6]These authors contributed equally

*Corresponding authors

A. A. Marusiak, IMol Polish Academy of Sciences, Flisa 6, Warsaw, 02-247, Poland

e-mail: a.marusiak@imol.institute

J. Brognard, National Cancer Institute, National Institutes of Health, Frederick, MD 21702, USA

e-mail: john.brognard@nih.gov

Page No	Content
S3	**Figure S1.** Evaluation of IAP- and CRBN-PROTACs.
S4	**Figure S2.** Specificity of endogenous MLK3 degradation by CEP1347-VHL-02 PROTAC in MCF-7 and MDA-MB-468 cell lines.
S5	**Figure S3.** Evaluation of different PROTACs by Western Blot analysis in MCF-7 and MDA-MB-468 cell lines.
S6	**Figure S4.** Shotgun proteomic analysis of total cell protein extracts from MCF-7 and MDA-MB-468 cell lines.
S7	**Figure S5.** Analysis of activation of JNK and ERK pathways in MCF-7 and MDA-MB-468 cell lines.
S8	**Figure S6.** Knock-down of MLK3 decreases the colony formation potential of MDA-MB-468, but not the MCF-7 cell line.
S9	**Figure S7.** Degradation of MLK3 by CEP1347-VHL-02 PROTAC treatment impaired the formation of MDA-MB-468 spheroids in 3D cell culture.
S10 – S32	**Figure S8.** NMR spectra and HPLC traces of newly synthesized PROTACs.

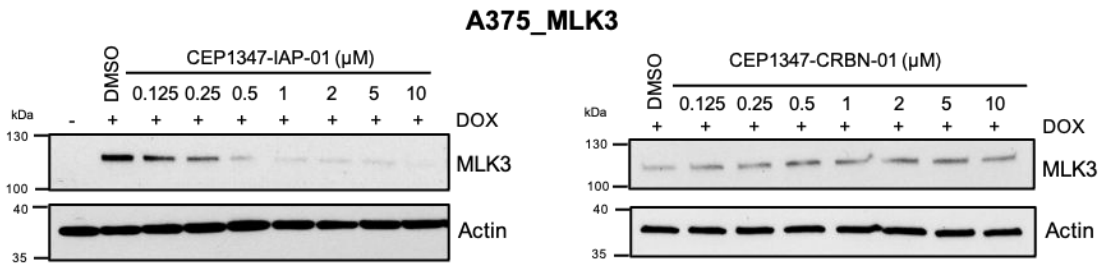

Figure S1. Evaluation of IAP- and CRBN-PROTACs. Western blot analysis of MLK3 levels in A375 cell line with doxycycline (DOX) inducible MLK3 overexpression after 24 h treatment with CEP1347-IAP-01 or CEP1347-CRBN-01 PROTACs in concentration ranges 0.125 μM - 10 μM. DMSO was used as a control.

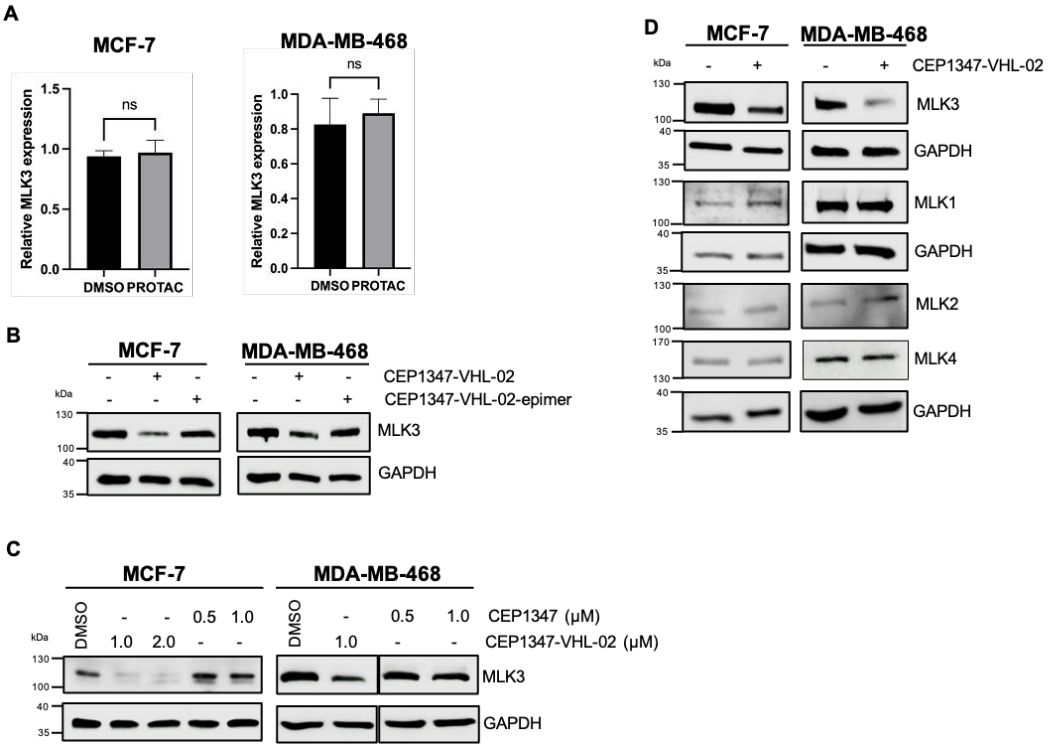

Figure S2. Specificity of endogenous MLK3 degradation by CEP1347-VHL-02 PROTAC in MCF-7 and MDA-MB-468 cell lines. (A) RT-qPCR analysis of MLK3 mRNA level in MCF-7 and MDA-MB-468 cell lines after 24 h treatment with 1 μM CEP1347-VHL-02 PROTAC. The results were normalized to GAPDH levels. (B) Western blot analysis of MLK3 levels in MCF-7 and MDA-MB-468 cell lines after 24 h treatment with 1 μM CEP1347-VHL-02 PROTAC or 1 μM CEP1347-VHL-02-epimer. DMSO was used as a control. (C) Western blot analysis of MLK3 levels in MCF-7 and MDA-MB-468 cell lines after 24 h treatment with CEP1347 compound or CEP1347-VHL-02 PROTAC. DMSO was used as a control. (D) Western blot analysis of MLK1, MLK2, MLK3 and MLK4 levels in MCF-7 and MDA-MB-468 cell lines after 24 h of 1 μM CEP1347-VHL-02 PROTAC treatment. DMSO was used as a control.

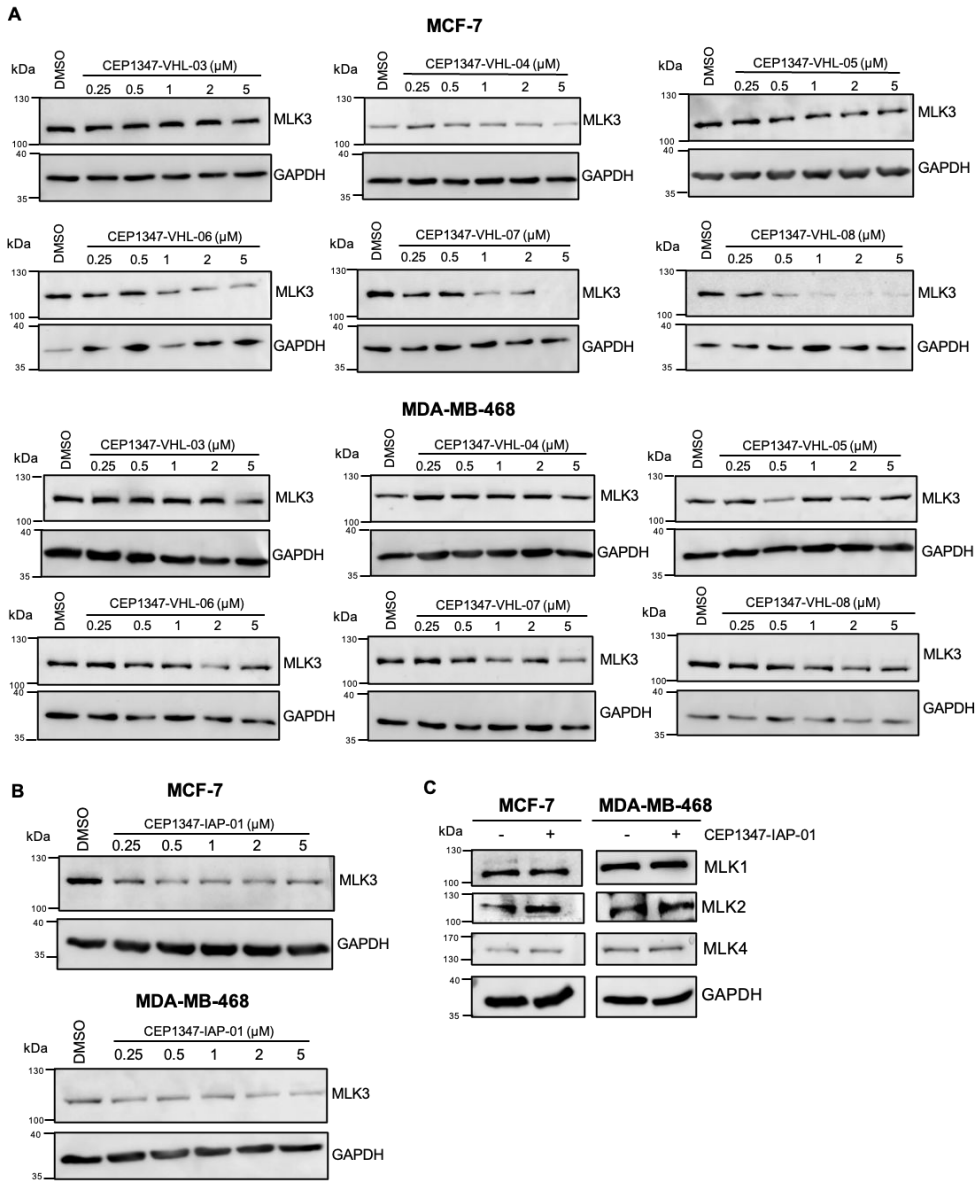

Figure S3. Evaluation of different PROTACs by Western Blot analysis in MCF-7 and MDA-MB-468 cell lines. (A) Western blot analysis of MLK3 levels in MCF-7 and MDA-MB-468 cell lines after 24 h treatment with different VHL-based PROTACs in concentration ranges 0.25 μM - 5 μM. DMSO was used as a control. (B) Western blot analysis of MLK3 levels in MCF-7 and MDA-MB-468 cell lines after 24 h treatment with CEP1347-IAP-01 PROTAC in concentration ranges 0.25 μM - 5 μM. DMSO was used as a control. (C) Western blot analysis of MLK1, MLK2 and MLK4 levels in MCF-7 and MDA-MB-468 cell lines after 24 h treatment with 1 μM CEP1347-IAP-01 PROTAC. DMSO was used as a control.

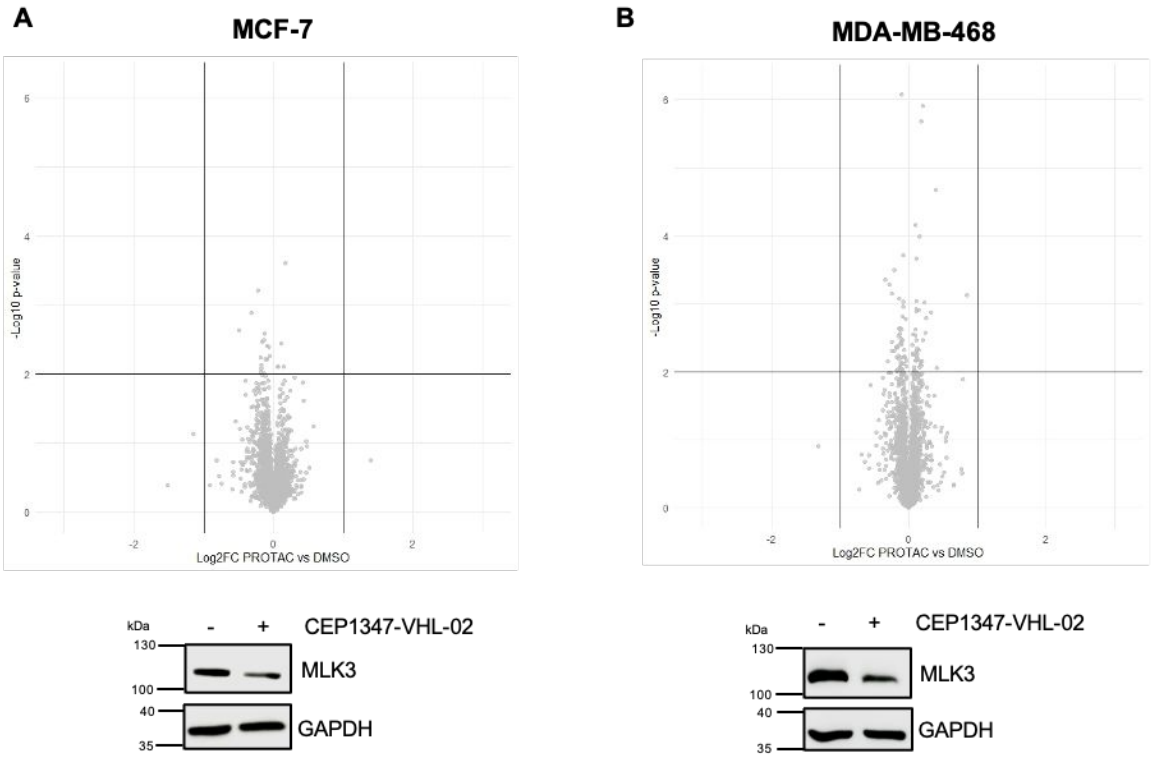

Figure S4. Shotgun proteomic analysis of total cell protein extracts from MCF-7 (A) and MDA-MB-468 (B) cell lines, and corresponding Western Blot analysis, after the treatment of 1 μM CEP1347-VHL-02 PROTAC for 24 hours.

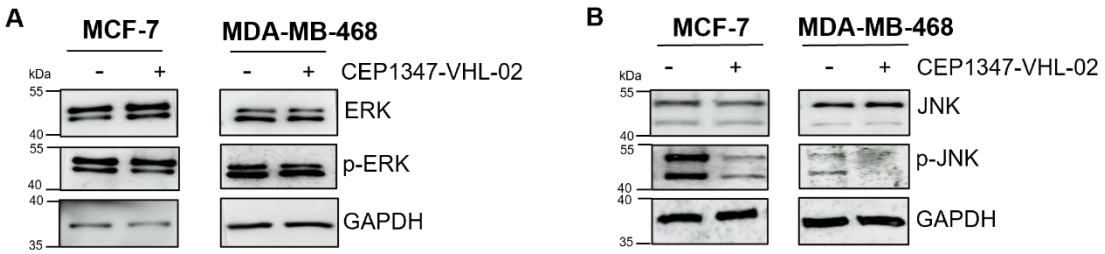

Figure S5. Degradation of MLK3 by CEP1347-VHL-02 PROTAC treatment decreased the activation of the JNK pathway, but not of the ERK pathway, in MCF-7 and MDA-MB-468 cell lines. (A) Western blot analysis of ERK and p-ERK in MCF-7 and MDA-MB-468 cell lines after 24 h of 1 μM CEP1347-VHL-02 PROTAC treatment. DMSO was used as a control. (B) Western blot analysis of JNK and p-JNK in MCF-7 and MDA-MB-468 cell lines after 24 h of 1 μM CEP1347-VHL-02 PROTAC treatment. DMSO was used as a control.

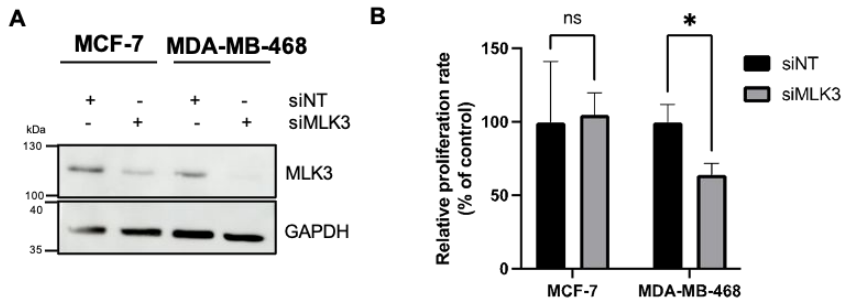

Figure S6. Knock-down of MLK3 decreases the colony formation potential of MDA-MB-468, but not the MCF-7 cell line. (A) MCF-7 and MDA-MB-468 cells were transiently transfected with siRNA targeting MLK3 or scrambled siRNA (siNT) as a control. Whole cell lysates were analyzed by Western blot. (B) Colony formation potential was assessed by crystal violet staining and quantified by absorbance measurement. The statistical analysis was performed using an unpaired *t*-test (*$p < 0.05$) compared with siNT control.

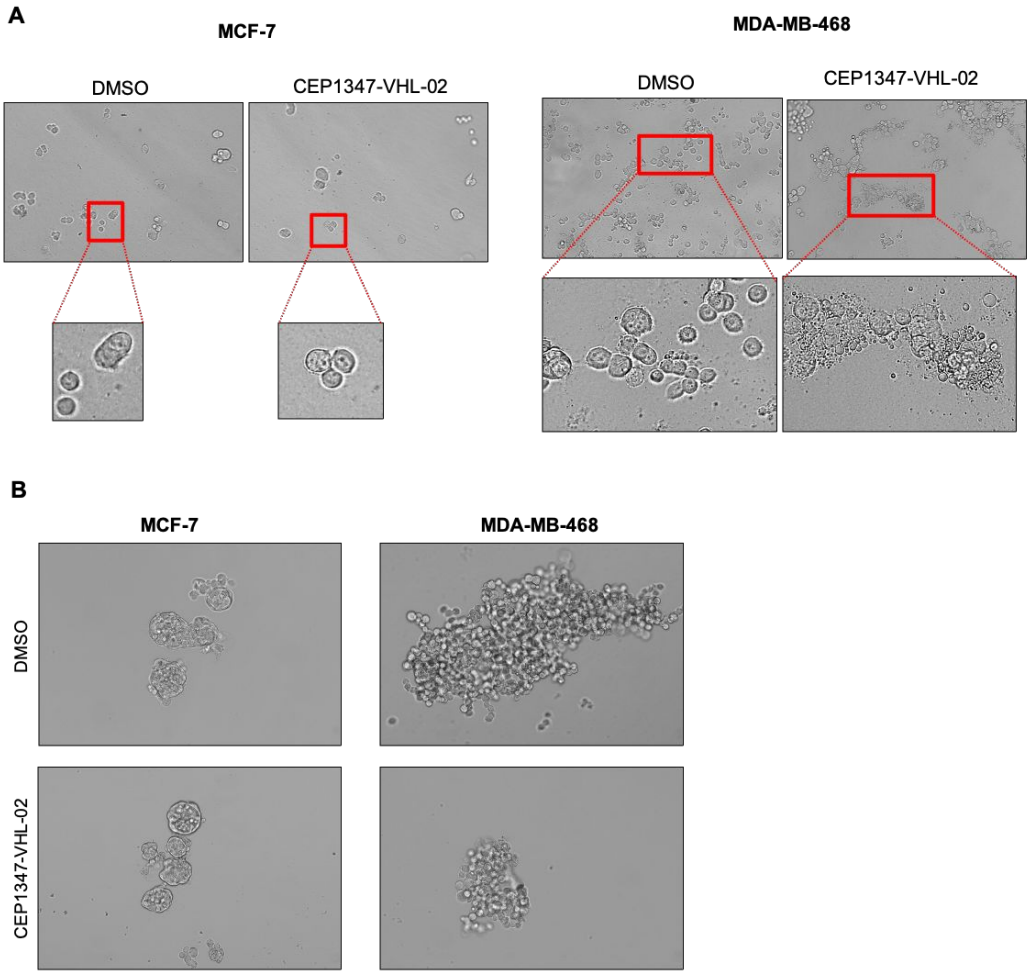

Figure S7. Degradation of MLK3 by CEP1347-VHL-02 PROTAC treatment impaired the formation of MDA-MB-468 spheroids in 3D cell culture. Representative photographs of spheroids formed by MCF-7 and MDA-MB-468 cells after 10 days of 1 μM CEP1347-VHL-02 PROTAC treatment in hydrogels (A) or low-attachment surface plates (B). DMSO was used as a control.

Figure S8. NMR spectra and HPLC traces of newly synthesized PROTACs.

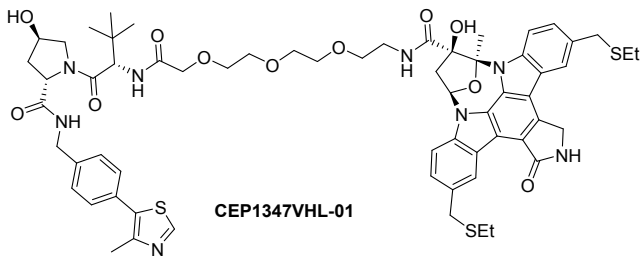

CEP1347VHL-01

CEP1347-VHL-01 ^{1}H NMR in DMSO-d$_6$

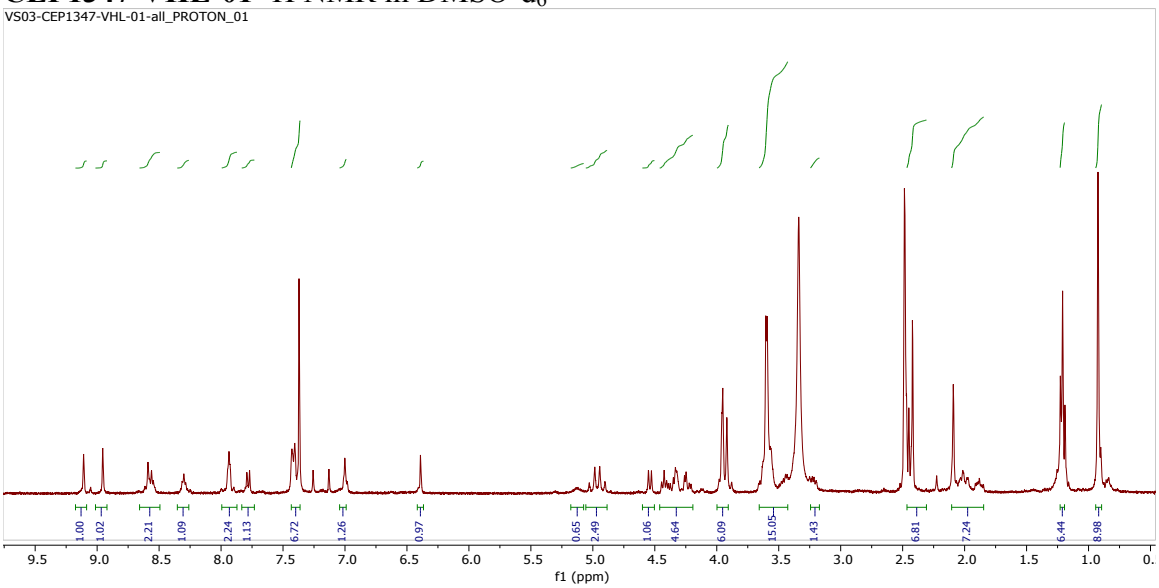

CEP1347-VHL-01 ^{13}C NMR in DMSO-d$_6$

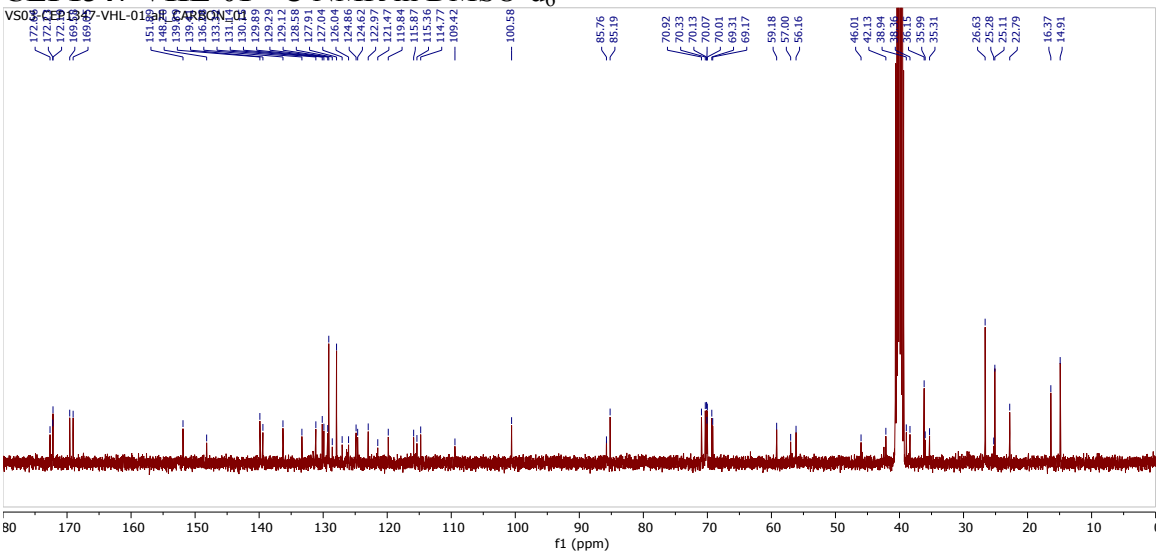

UPLC-MS of **CEP1347-VHL-01**

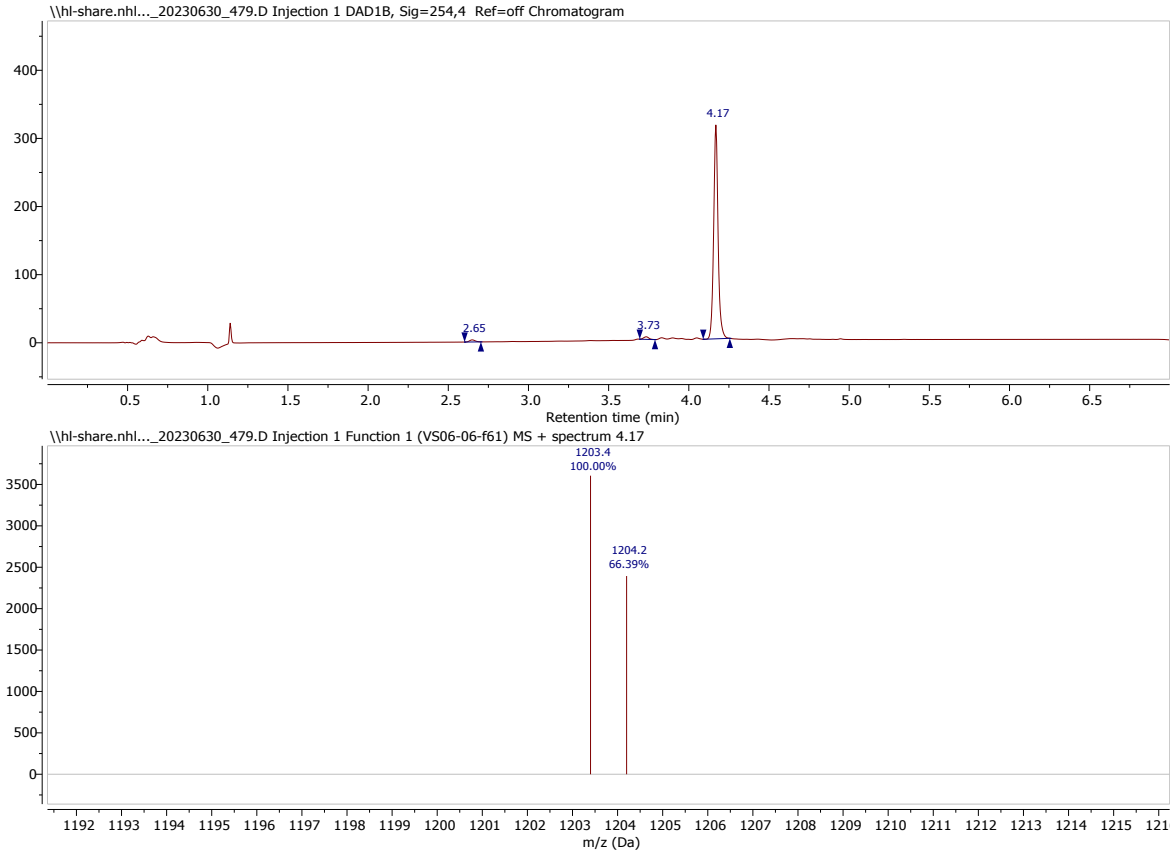

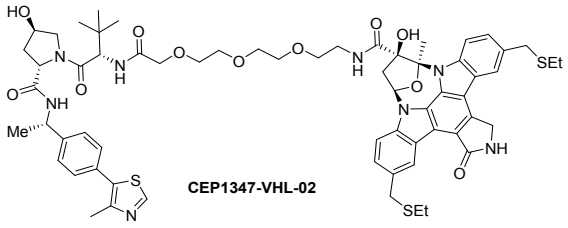

CEP1347-VHL-02 ^{1}H NMR in $CDCl_3$

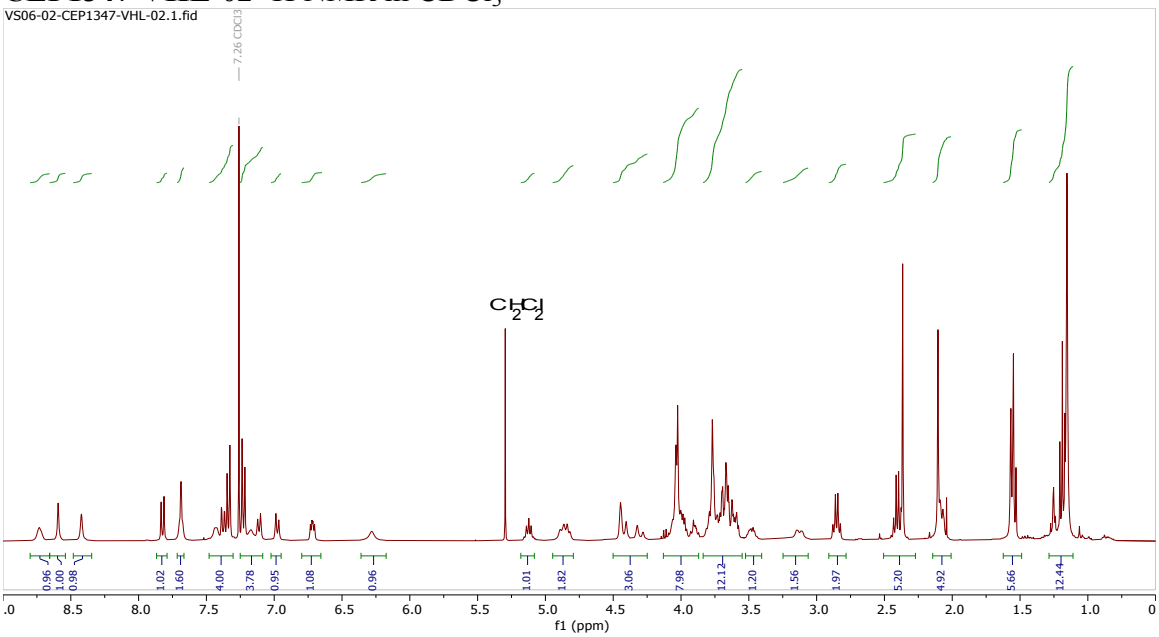

CEP1347-VHL-02 ^{13}C NMR in $CDCl_3$

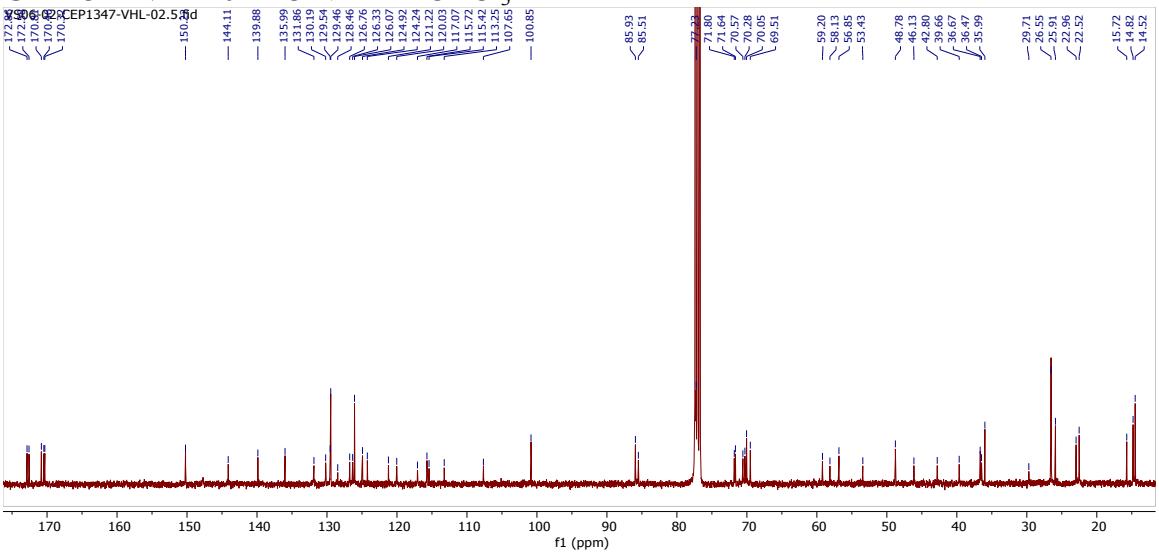

UPLC-MS of **CEP1347-VHL-02**

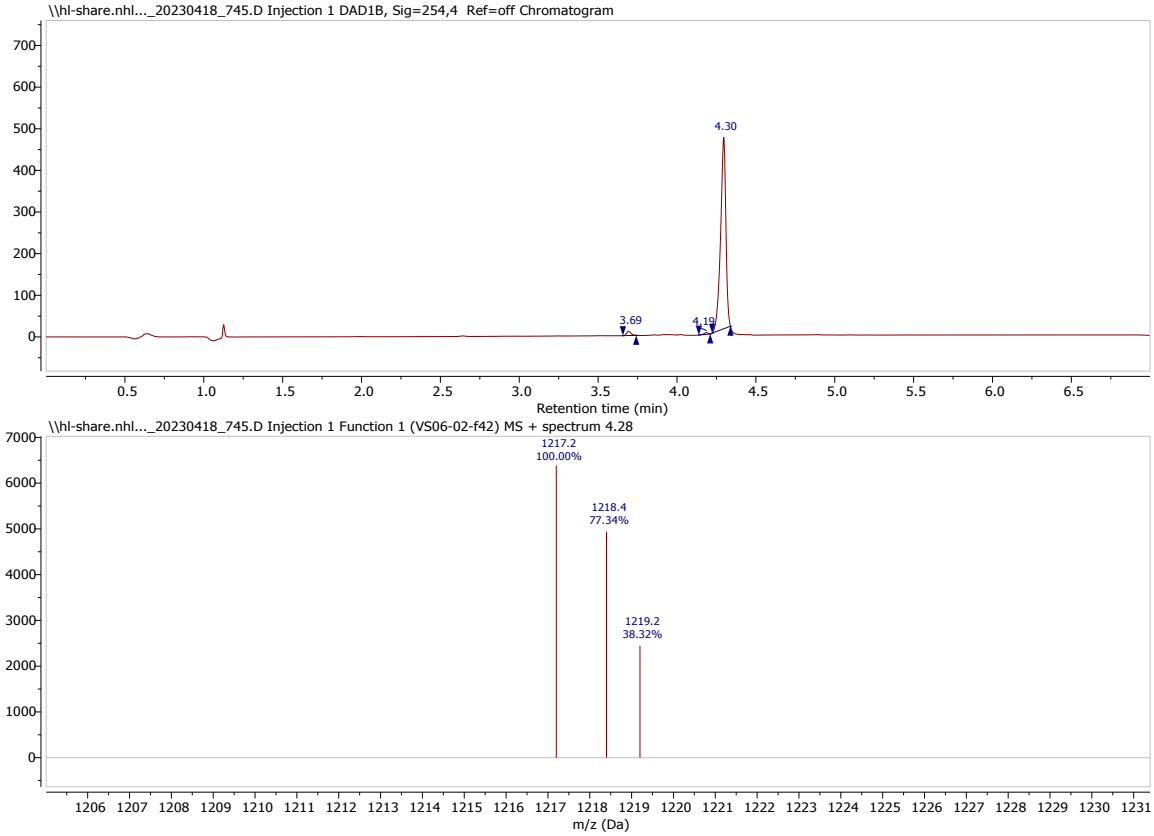

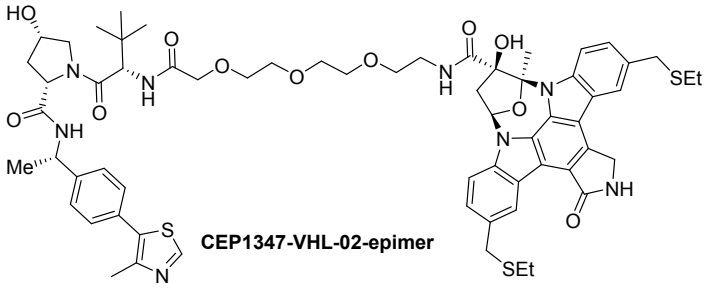

CEP1347-VHL-02-epimer

CEP1347-VHL-02-epimer ^{1}H NMR in $CDCl_3$

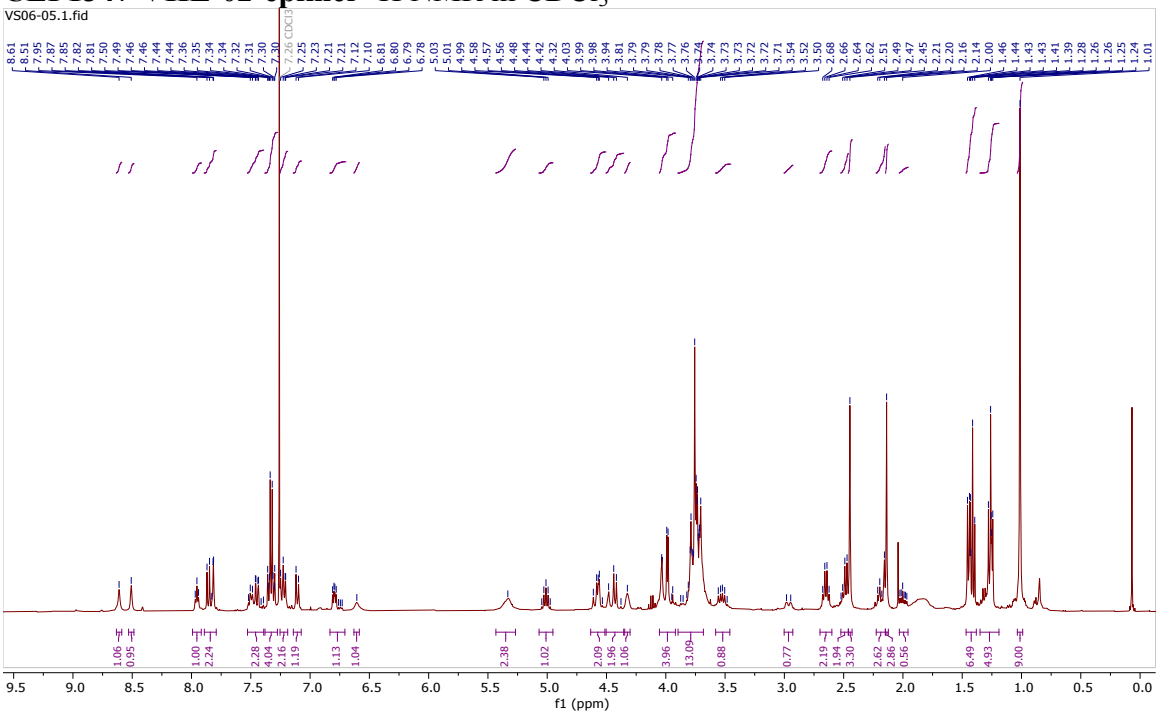

CEP1347-VHL-02-epimer ^{13}C NMR in $CDCl_3$

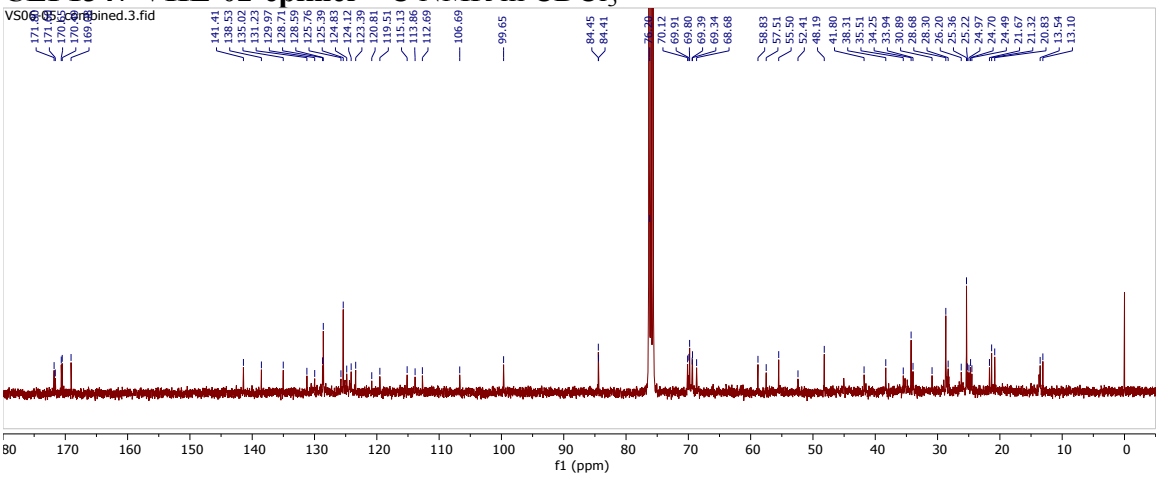

UPLC-MS of **CEP1347-VHL-02-epimer**

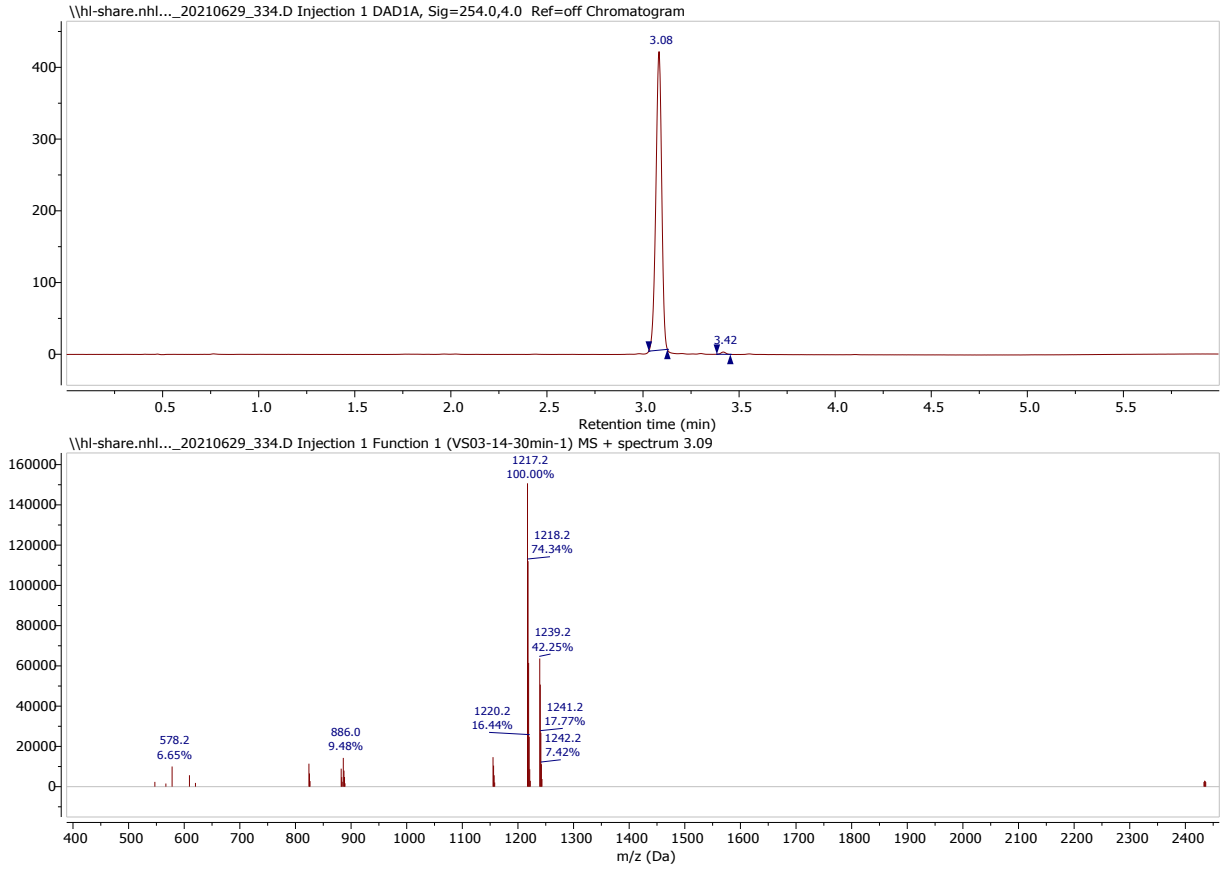

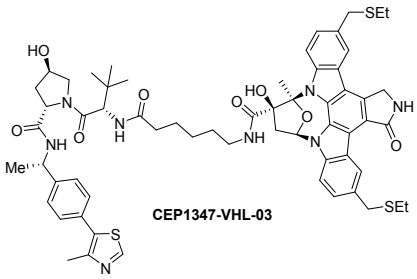

CEP1347-VHL-03 ^{1}H NMR in DMSO-d$_6$

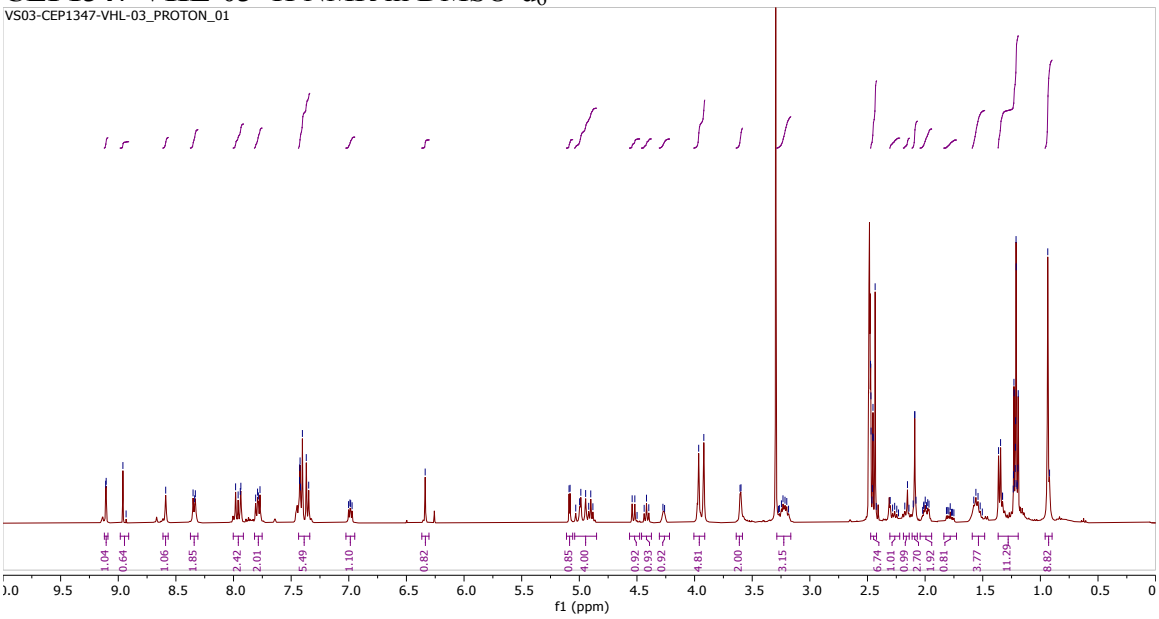

CEP1347-VHL-03 ^{13}C NMR in DMSO-d$_6$

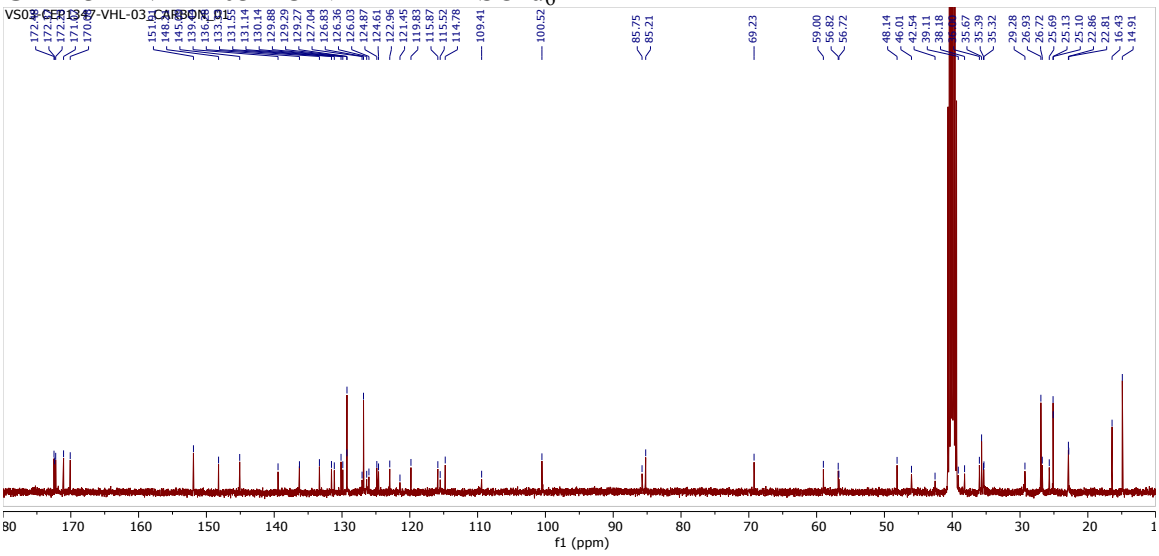

UPLC-MS of **CEP1347-VHL-03**

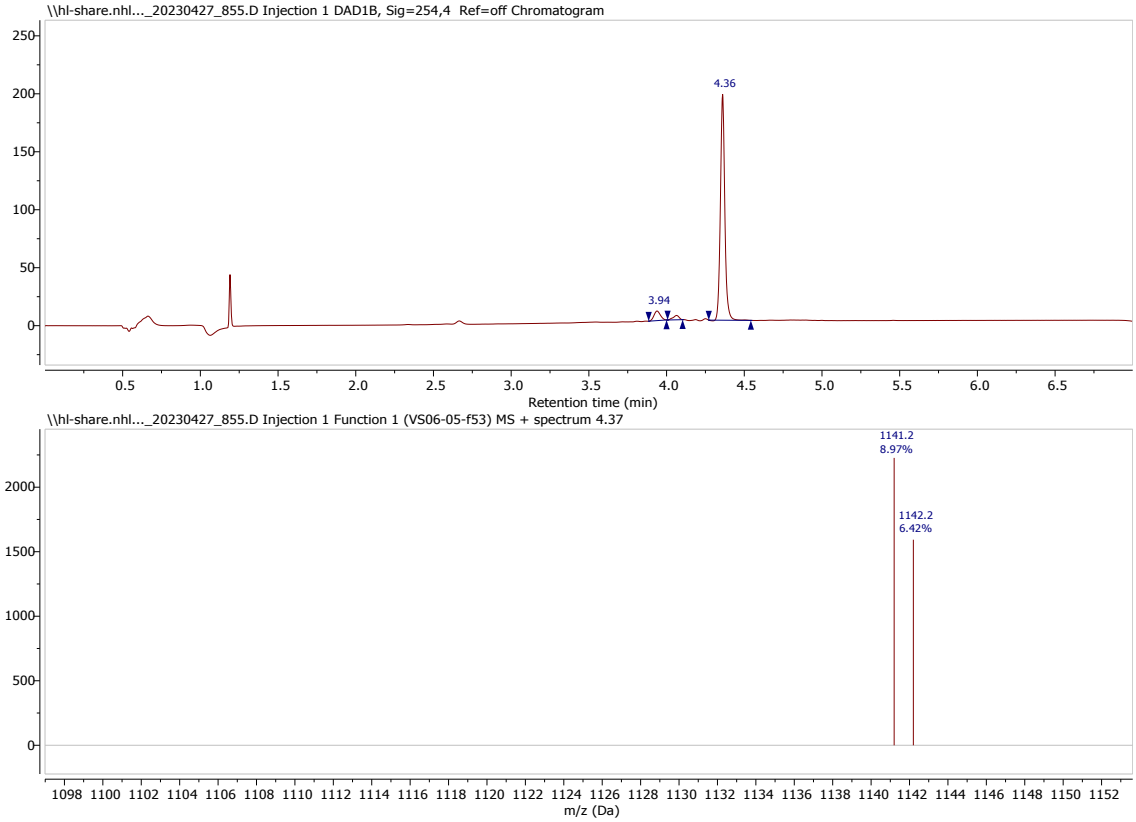

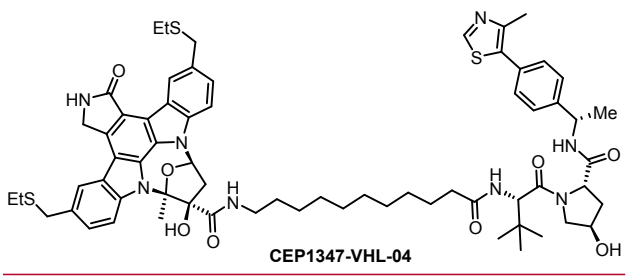

CEP1347-VHL-04

CEP1347-VHL-04 ^{1}H NMR in $CDCl_3$

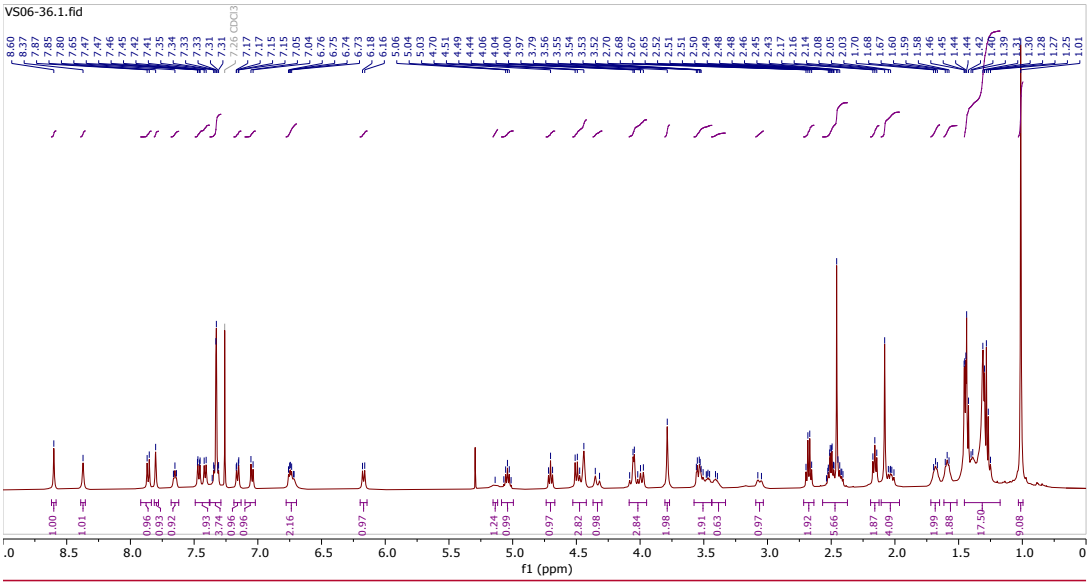

CEP1347-VHL-04 ^{13}C NMR in $CDCl_3$

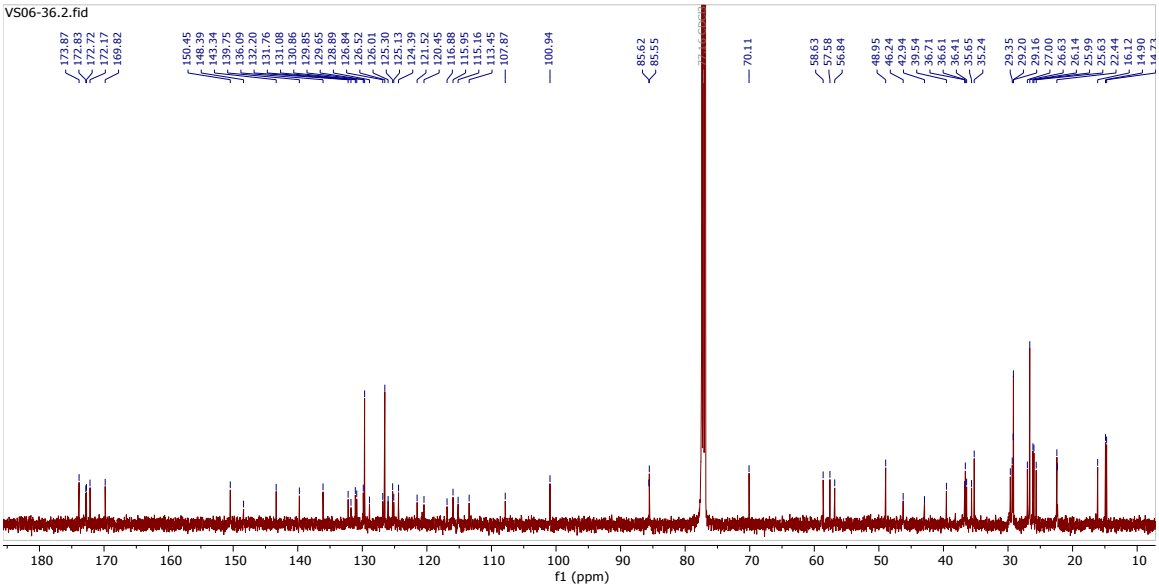

UPLC-MS of **CEP1347-VHL-04**

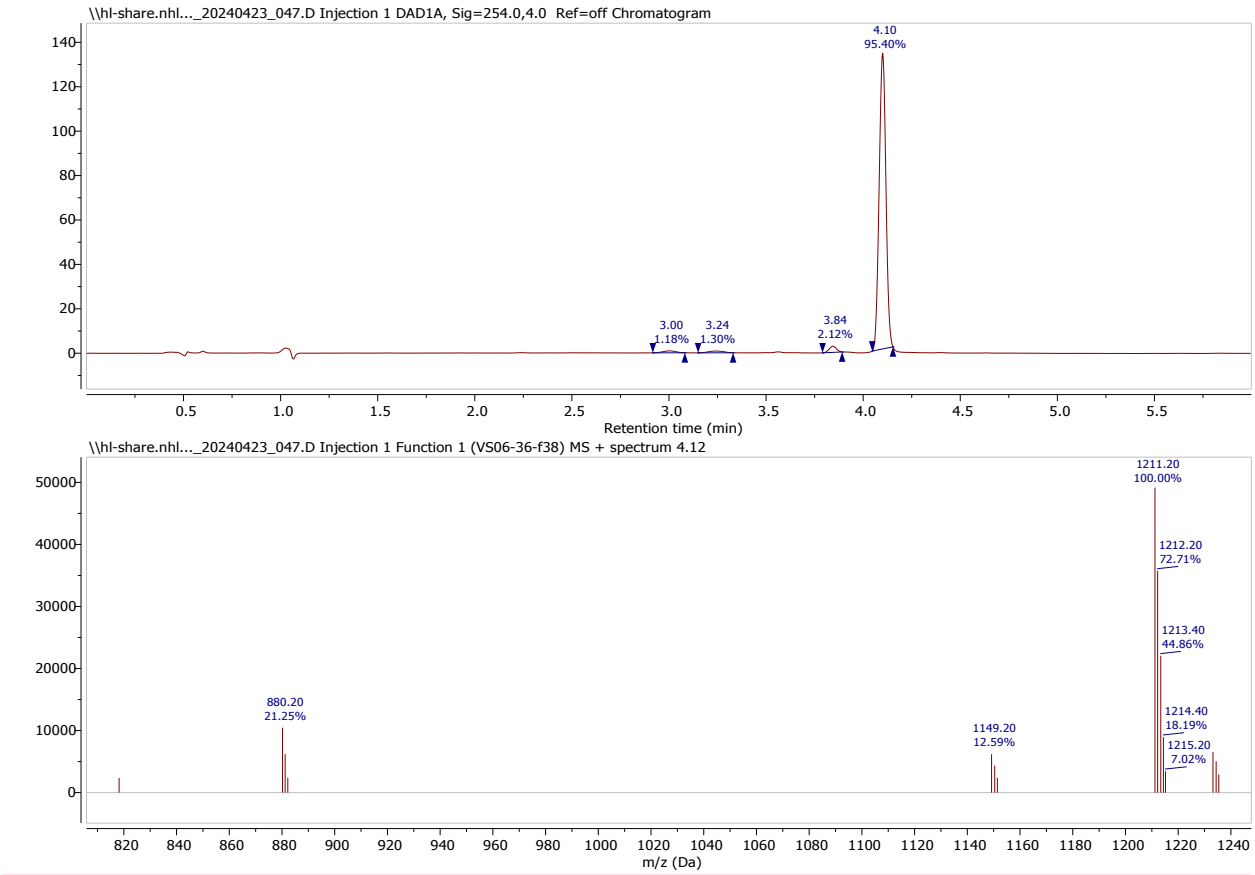

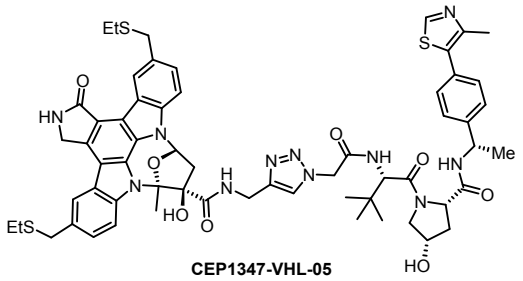

CEP1347-VHL-05

CEP1347-VHL-05 ^{1}H NMR in DMSO-d$_6$

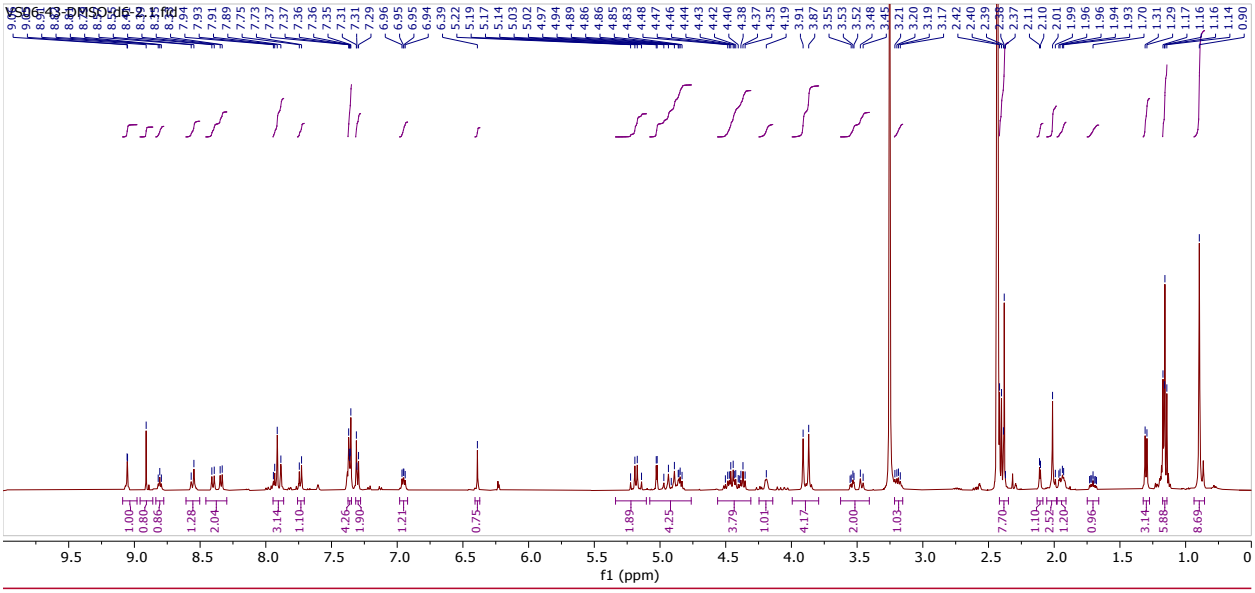

CEP1347-VHL-05 ^{13}C NMR in DMSO-d$_6$

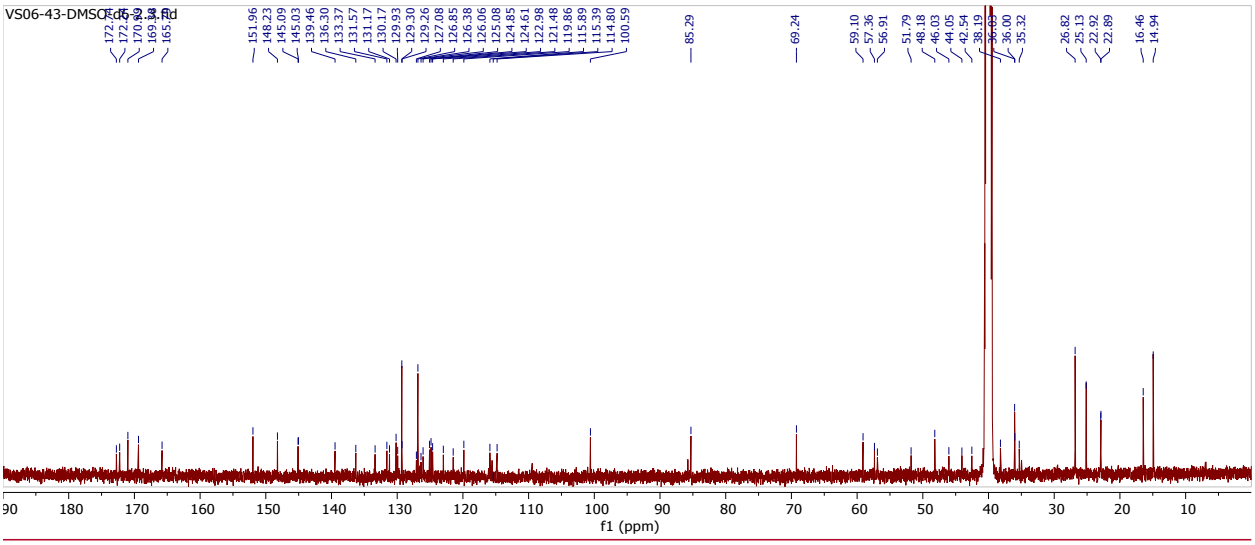

UPLC-MS of **CEP1347-VHL-05**

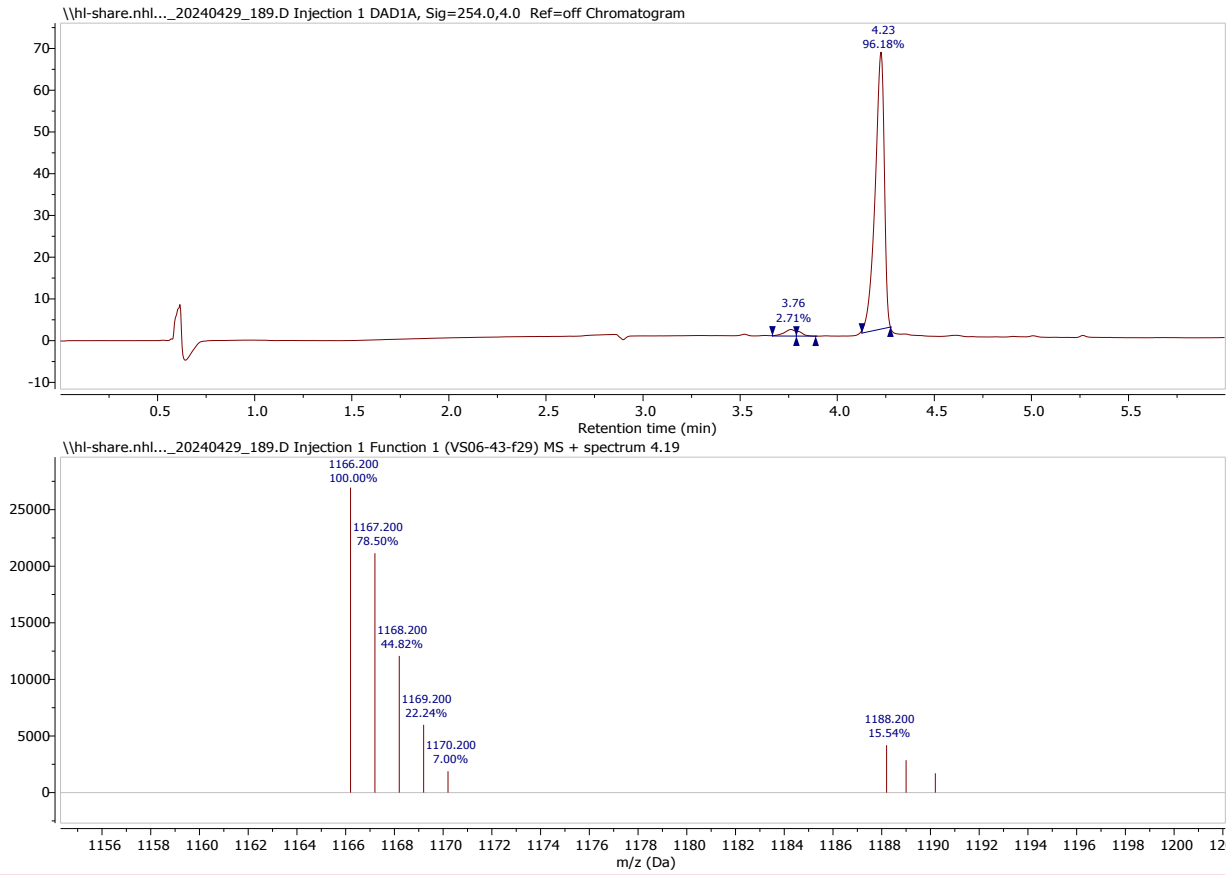

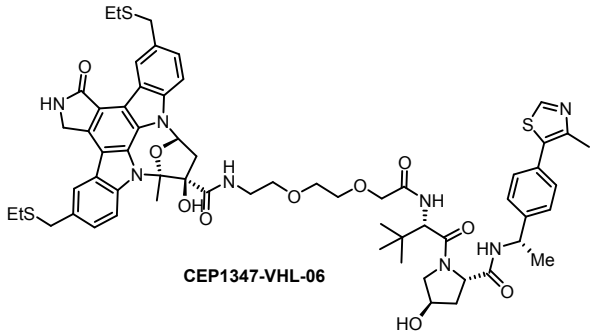

CEP1347-VHL-06

CEP1347-VHL-06 ^{1}H NMR in DMSO-d$_6$

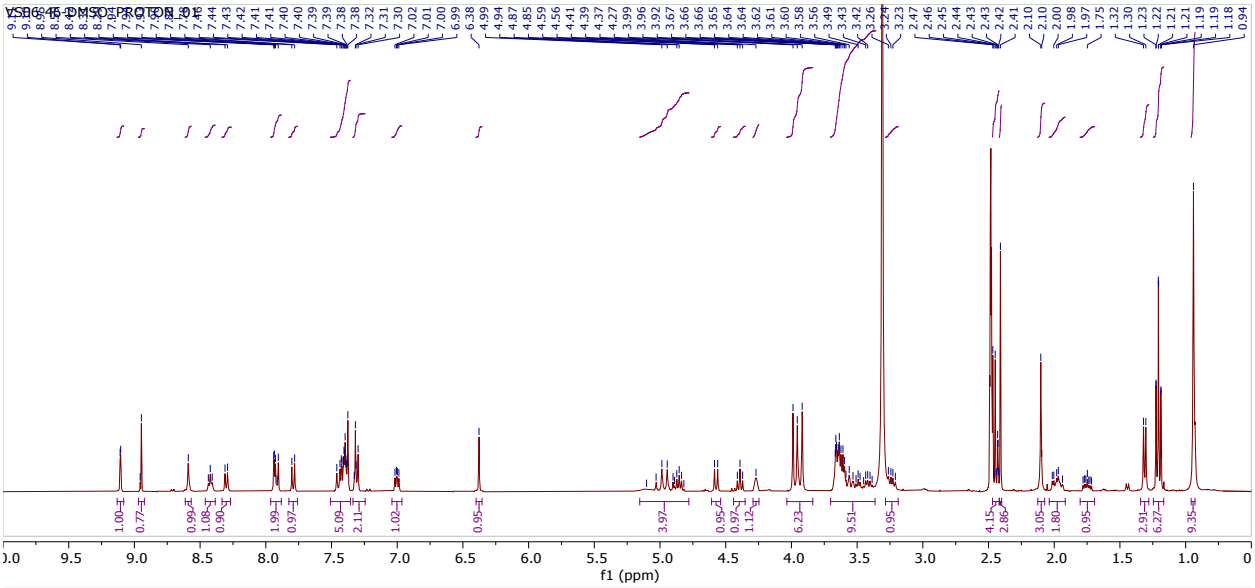

CEP1347-VHL-06 ^{13}C NMR in DMSO-d$_6$

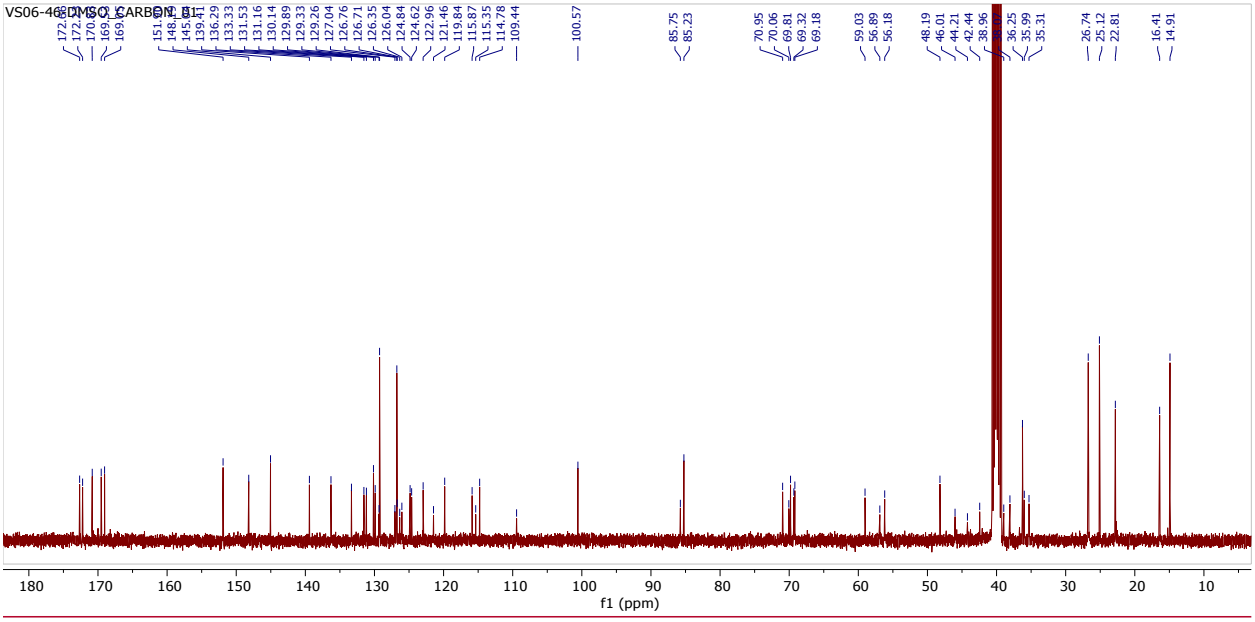

UPLC-MS of **CEP1347-VHL-06**

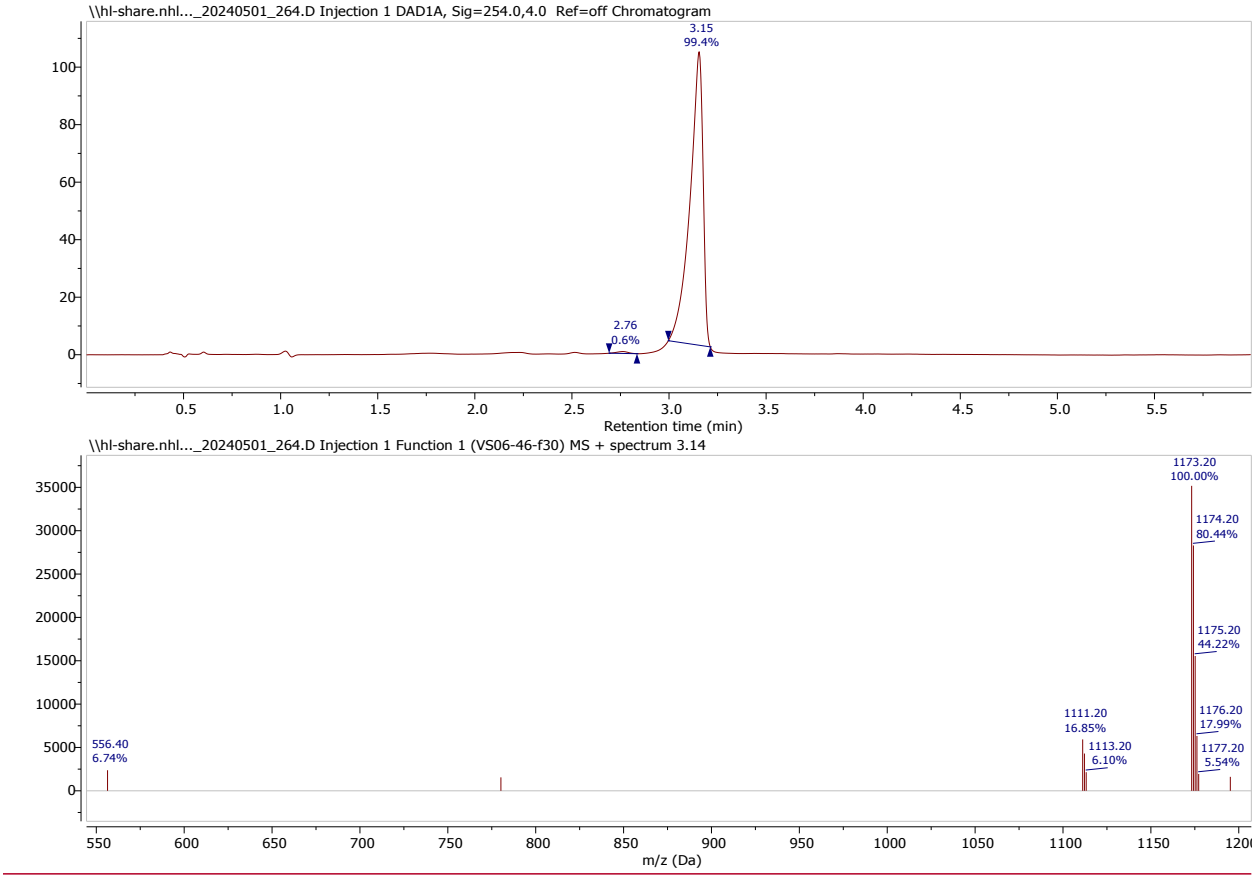

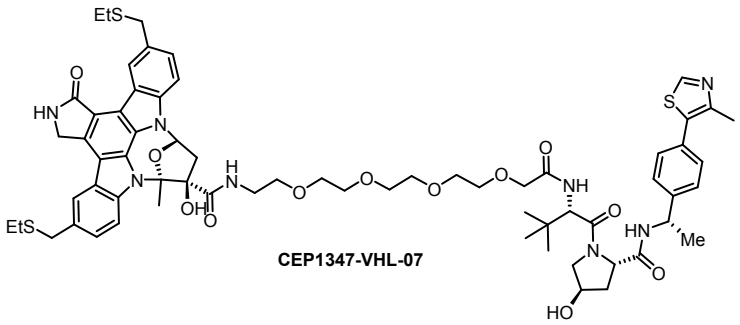

CEP1347-VHL-07

CEP1347-VHL-07 ^{1}H NMR in $CDCl_3$

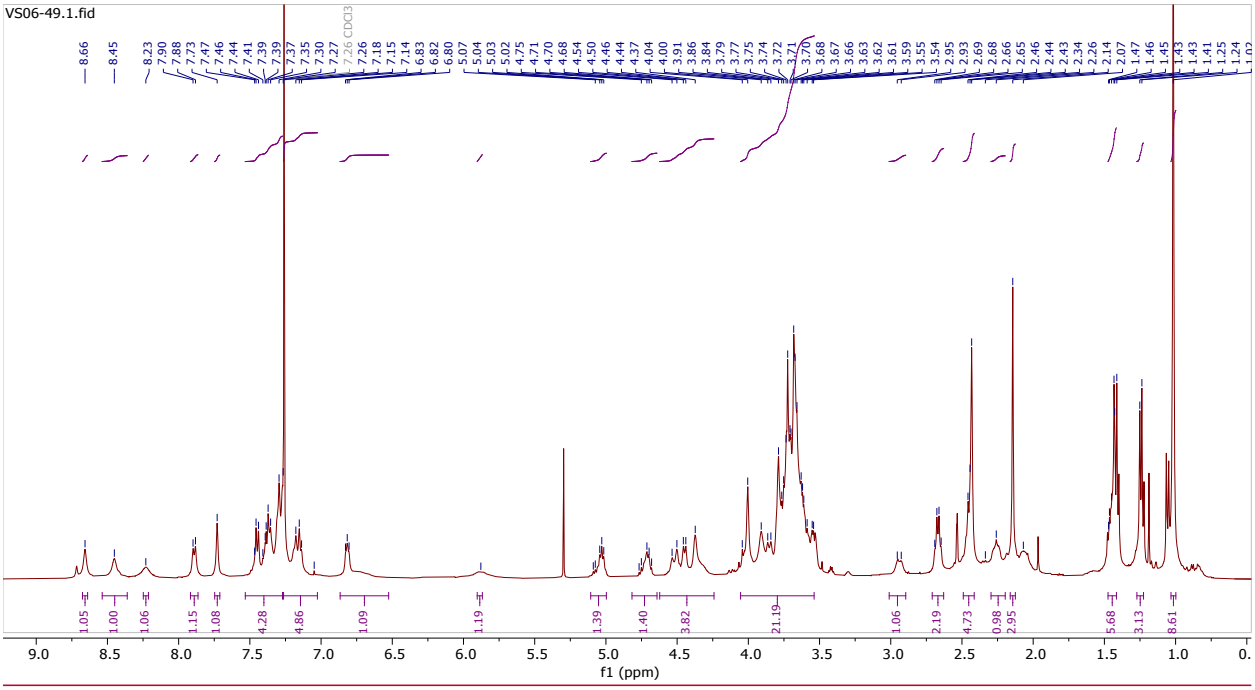

CEP1347-VHL-07 ^{13}C NMR in $CDCl_3$

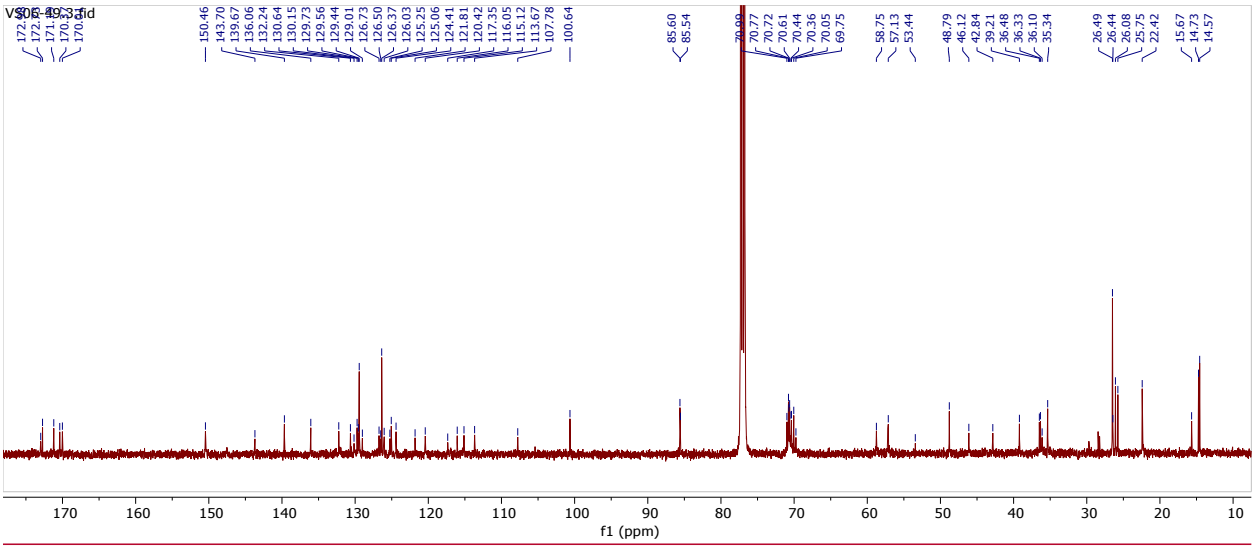

UPLC-MS of **CEP1347-VHL-07**

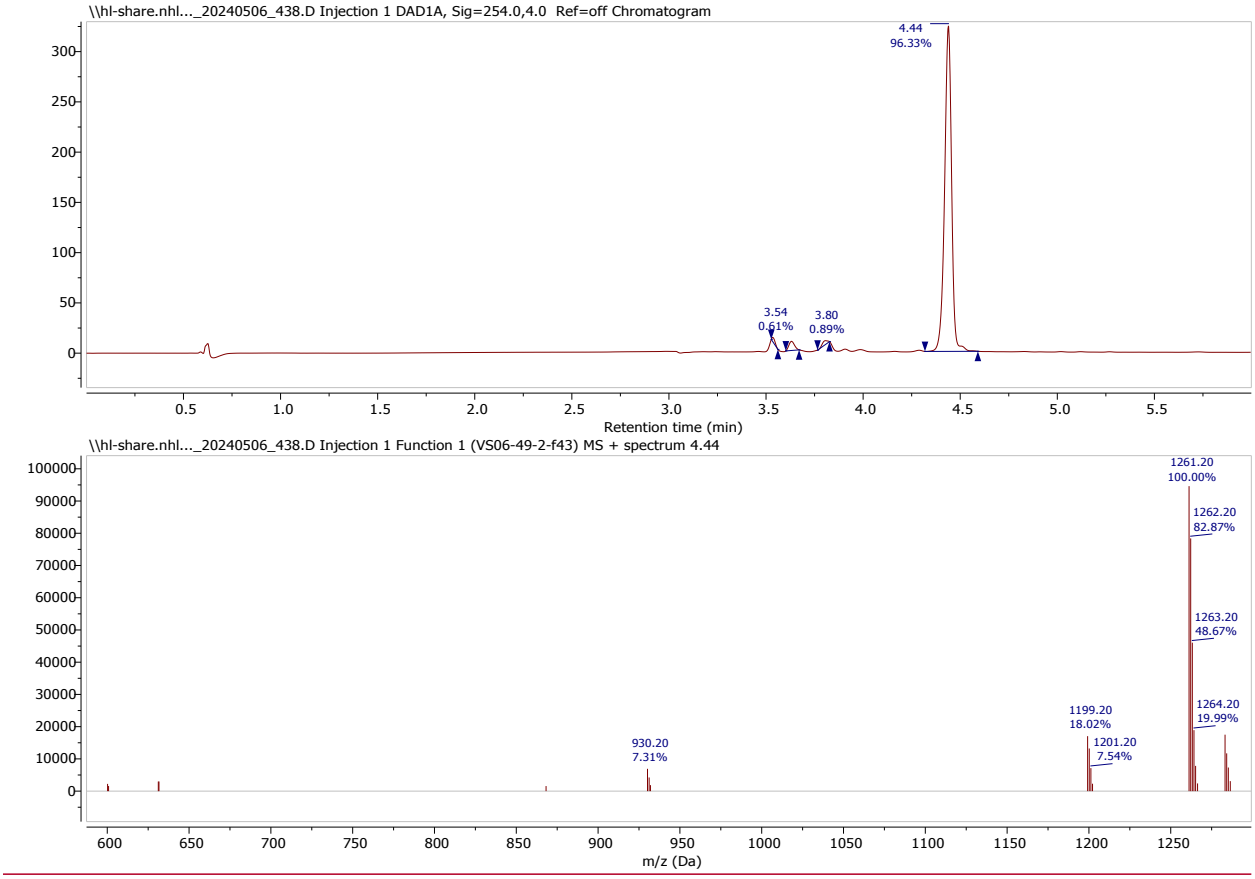

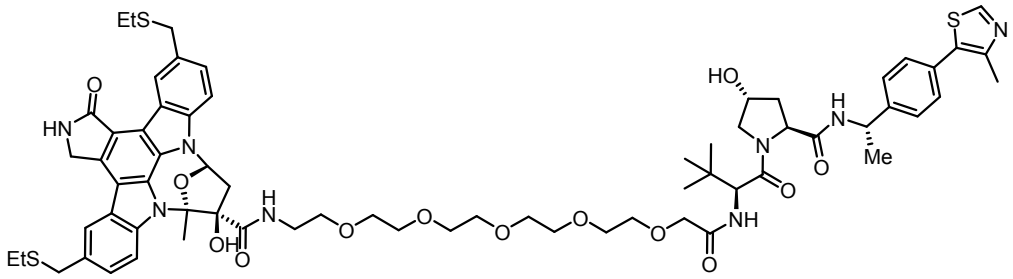

CEP1347-VHL-08

CEP1347-VHL-08 ^{1}H NMR in DMSO-d_6

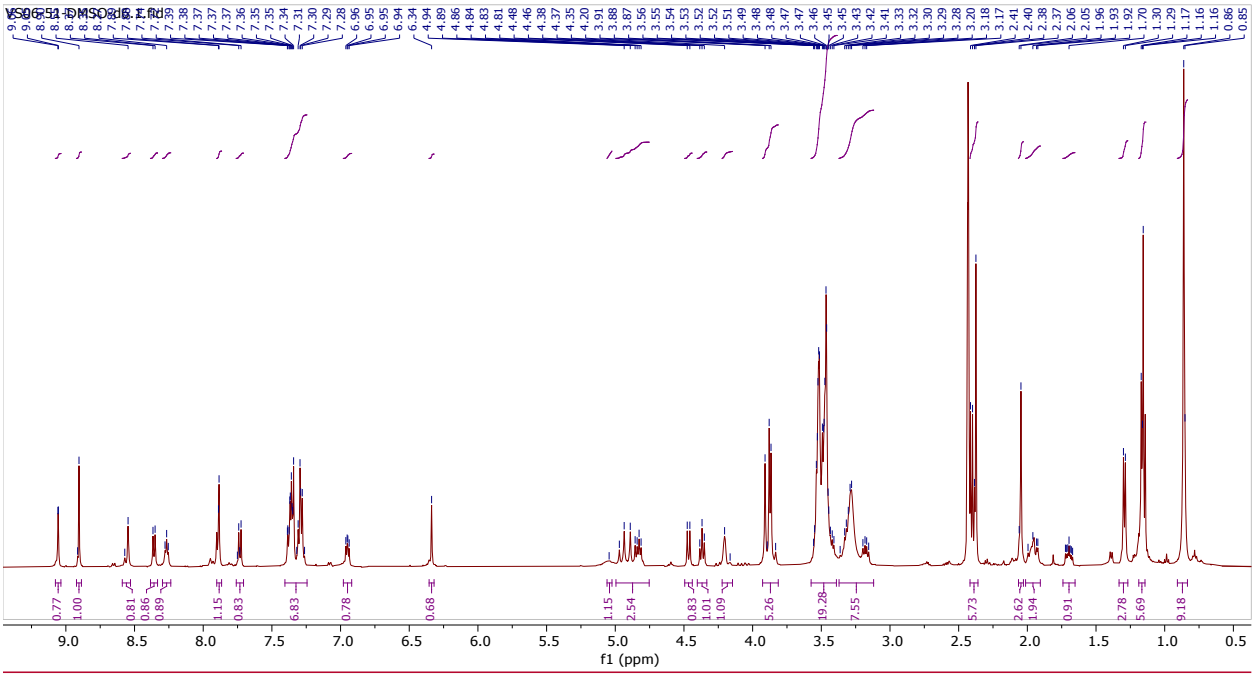

CEP1347-VHL-08 ^{13}C NMR in DMSO-d_6

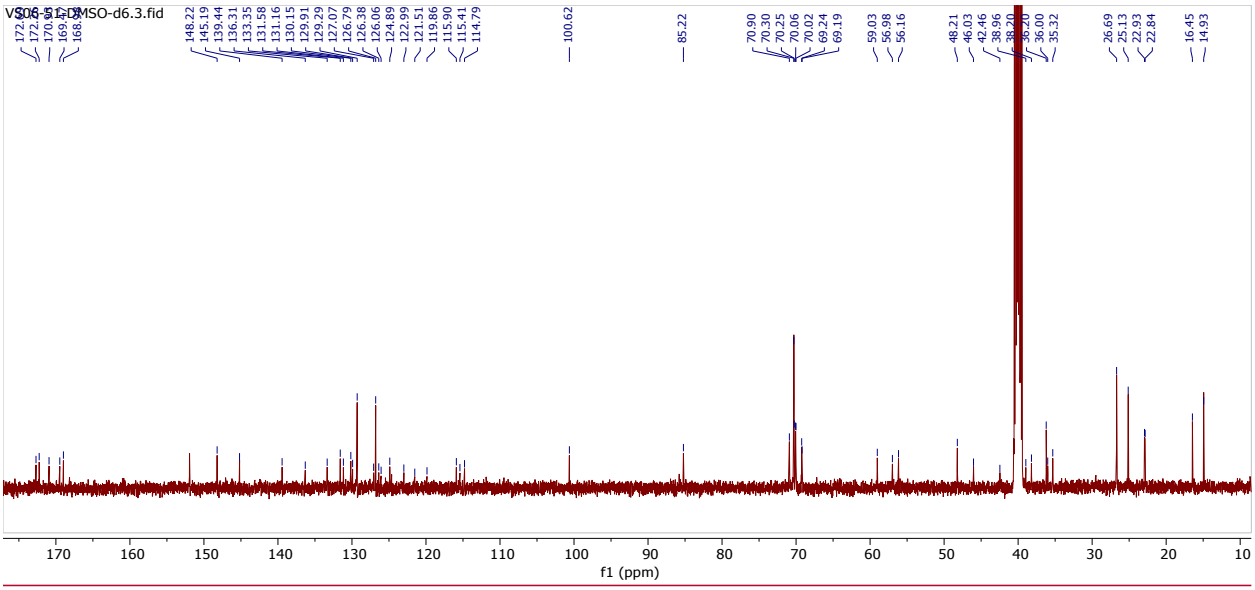

UPLC-MS of **CEP1347-VHL-08**

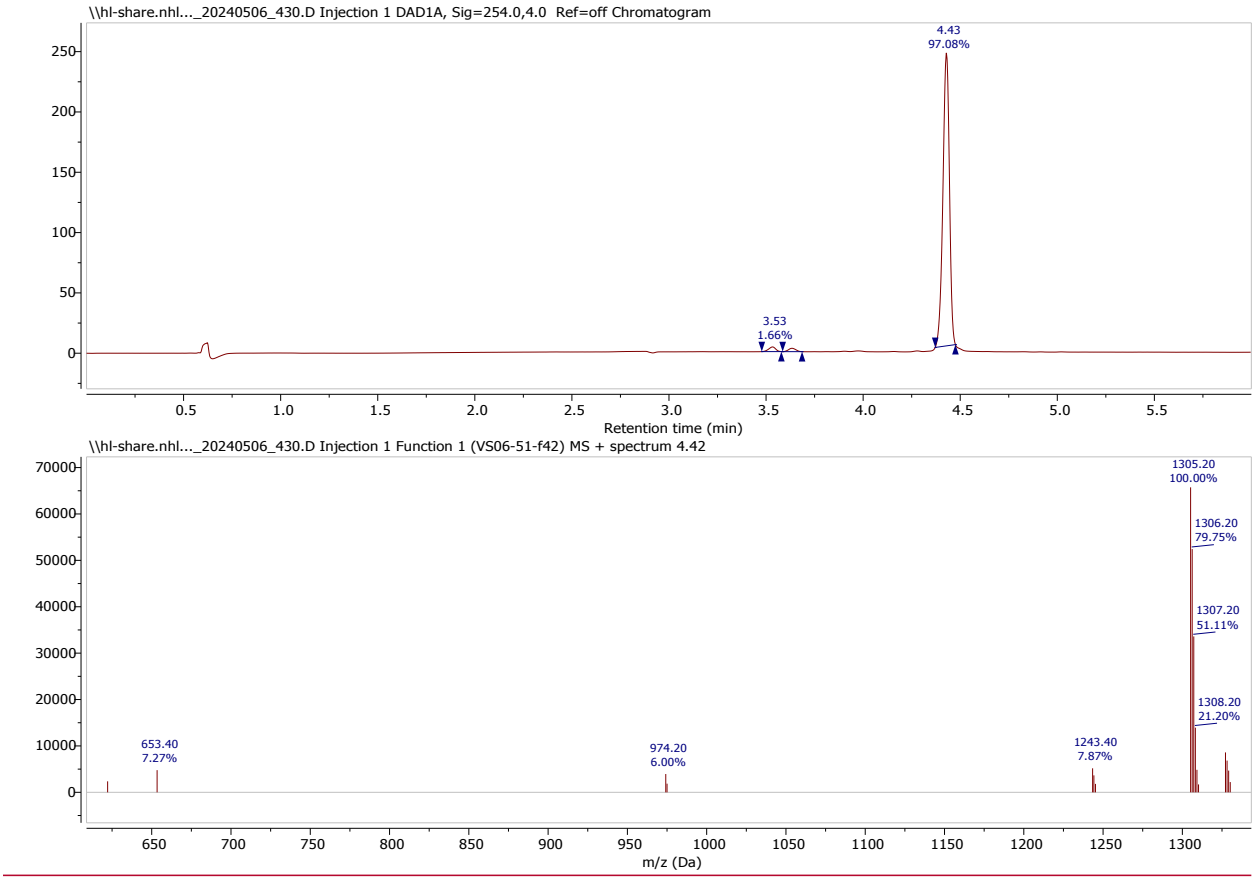

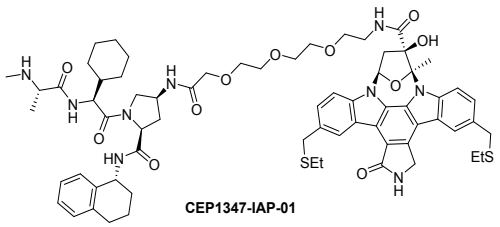

CEP1347-IAP-01 ^{1}H NMR in DMSO-d_6

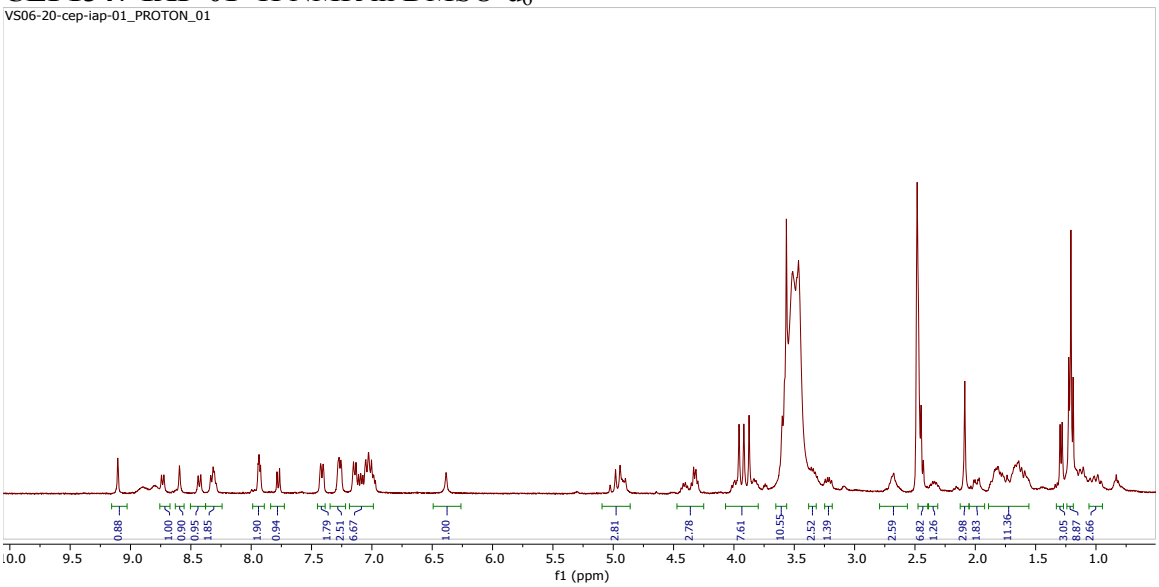

CEP1347-IAP-01 ^{13}C NMR in DMSO-d_6

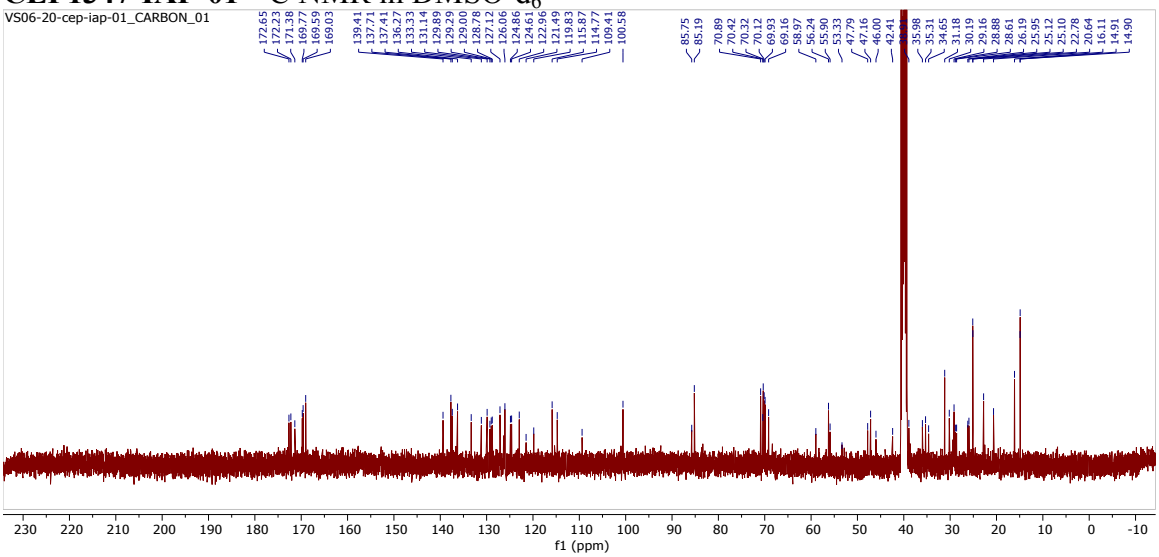

UPLC-MS of **CEP1347-IAP-01**

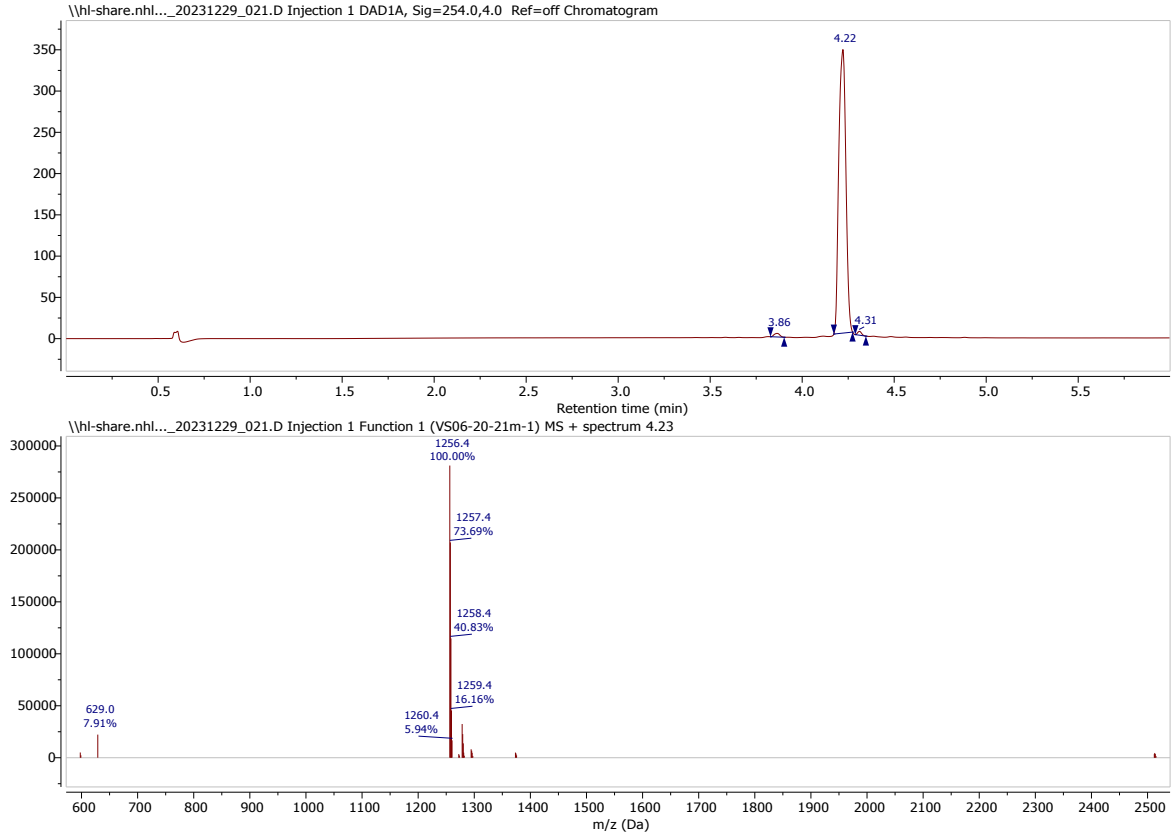

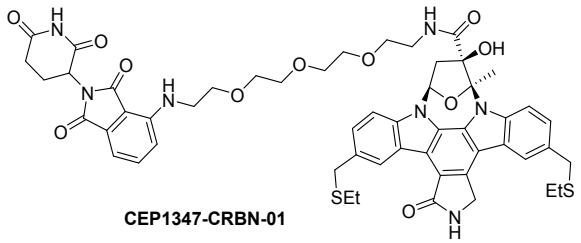

CEP1347-CRBN-01 ^{1}H NMR in DMSO-d$_6$

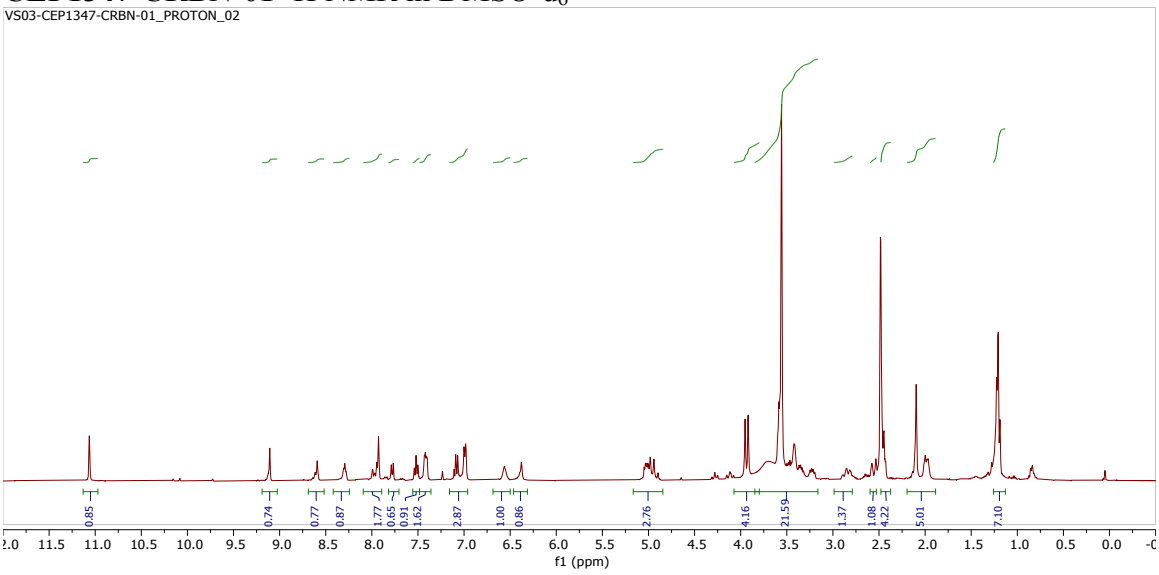

CEP1347-CRBN-01 ^{13}C NMR in DMSO-d$_6$

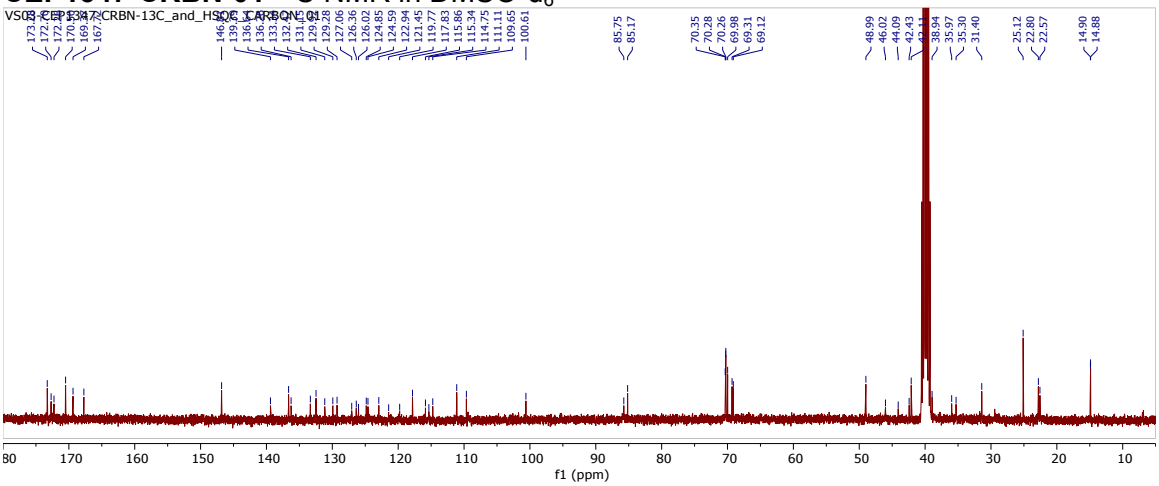

UPLC-MS of **CEP1347-CRBN-01**